

Efficient and Exact Multimarginal Optimal Transport with Pairwise Costs*

Bohan Zhou[†] and Matthew Parno[‡]

Abstract. In this paper, we address the numerical solution to the multimarginal optimal transport (MMOT) with pairwise costs. MMOT, as a natural extension from the classical two-marginal optimal transport, has many important applications including image processing, density functional theory and machine learning, but yet lacks efficient and exact numerical methods. The popular entropy-regularized method may suffer numerical instability and blurring issues. Inspired by the back-and-forth method introduced by Jacobs and Léger, we investigate MMOT problems with pairwise costs. First, such problems have a graphical representation and we prove equivalent MMOT problems that have a tree representation. Second, we introduce a novel algorithm to solve MMOT on a rooted tree, by gradient based method on the dual formulation. Last, we obtain accurate solutions which can be used for the regularization-free applications.

Key words. Multimarginal optimal transport, tree structure, graphical representation, back-and-forth method.

AMS subject classifications (2020). 49Q22, 65K10, 49M29, 49N15, 90C35.

1. Introduction. Probability distributions are used throughout statistics, machine learning, and applied mathematics to model complex datasets and characterize uncertainty. Quantitatively comparing distributions and identifying structure in the space of probability distributions are therefore fundamental components of many modern algorithms for data analysis. Optimal transport (OT) provides a natural way of comparing two distributions, often referred as marginals, by measuring how much effort is required to transform one distribution into another. The solution of an OT problem provides both a distance, called the *Wasserstein distance*, and a joint distribution, called the *optimal coupling*, which describes the optimal mass allocation between marginals. Multi-marginal optimal transport (MMOT), which is the focus of this effort, provides a generalization to situations with more than two marginals.

The field of OT has existed since Monge in the late 18th century, but has reemerged over the last few decades as a powerful theoretical and computational tool in many areas. Applications can be found in fields as diverse as chemistry and materials science [PR09, DBCC16, XZ21], geophysics [YESH18, PWS⁺19], image processing [SKA15, BCC⁺15, SDGP⁺15], fluid dynamics [Bre89, BB00, Bre08], and machine learning [FZM⁺15, CFHR17, ACB17, GPC18, CMM⁺20], to name just a few. A key contributor to this surge is the development of efficient numerical methods for approximately solving OT problems. The concept of regularized optimal transport received renewed attention following [Cut13], where an entropy regularization term is added to the original optimal transport problem, to form a matrix scaling problem that can be efficiently solved with Sinkhorn iterations [SK67]. The result is an easy-to-compute, albeit approximate, solution to the optimal transport problem.

Many refinements and extensions of regularized optimal transport have since been de-

*August, 2022.

Funding: ONR MURI #N00014-20-1-2595.

[†]Department of Mathematics, Dartmouth College, Hanover, NH, USA (Bohan.Zhou@Dartmouth.edu).

[‡]Department of Mathematics, Dartmouth College, Hanover, NH, USA (Matthew.D.Parno@Dartmouth.edu)

veloped (e.g., [DPR18, CP18, Sch19]) including GPU-accelerated implementations [FSV⁺19], but the computational expense of these approaches can still become significant for small levels of entropic regularization. This makes such approaches intractable on quantitative applications where accurate approximations of the unregularized optimal coupling are required. For example, when the application demands maintaining the fluid dynamics interpretation of optimal transport [BB00], as it does in the sea ice velocity estimation problem of [PWS⁺19]. In addition, regularized formulations result in diffuse couplings that also cause blurring in image processing like barycentric interpolation [BCC⁺15].

The exact (unregularized) solution to OT is currently only feasible for certain subclasses of OT. OT on discrete measures is fundamentally an assignment problem and can be formulated as linear programming (LP). If the number of Dirac masses in the discrete measures is not too large, LP can be solved directly. Semi-discrete OT, where one measure is discrete and the other is continuous, is also naturally cast as a finite dimensional optimization problem (e.g., [MM16, KMT19]) and can often be solved exactly. Continuous OT problems, where both measures admit densities with respect to the Lebesgue measure, admit a PDE formulation based on the Monge-Ampère equation, which can be solved efficiently in 2 or 3 dimensions to obtain the OT solution [BFO14]. The authors of [JL20] also provide an alternative method for OT with continuous distributions that can be represented on a uniform grid in \mathbb{R}^d . Their approach, called the “back-and-forth method” (BFM), lays the foundations for our MMOT solver and will be discussed in more detail in [subsection 2.4](#).

The MMOT problem has different theoretical properties than the classic two-marginal OT problem. Please refer to [Pas15] for a detailed theoretical survey and [PVJ21] for some interesting examples. Many important applications, for example, the Wasserstein barycenter [AC11] and the adversarial multiclass classification [TJK22], are in the form of MMOT. There is, however, a lack of efficient computational techniques for the exact solution to MMOT.

Analogously with the entropy regularized OT, there are algorithms to solve the entropy regularized MMOT [BCC⁺15, EHJK20, HRCK21, FHKC22]. However, they in general suffer the same numerical instability and blurring issues as the regularized OT. The approach of [NX22] provides a regularization-free alternative for approximately solving MMOT problems with controllable levels of sub-optimality. However, the scalability of this approach to higher dimensional spaces with complex marginals is unclear. Our goal is to construct a fast and exact (to within numerical tolerances) MMOT solver that can scale to marginal distributions derived from high resolution imagery.

Contribution. In this paper, we develop and analyze a novel algorithm for the efficient solution of continuous MMOT problems with pairwise costs. More specifically, our method can deal with all cost function in a pairwise form $c(x_1, \dots, x_m) = \sum_{i < j} c_{ij}(x_i, x_j)$, which includes most classical cost functions used in MMOT except for the determinant form of [CN08]. In this category of cost functions, there is a natural graphical structure between marginals that our approach exploits to construct an efficient MMOT solver. In particular, inspired by the “back-and-forth” method of [JL20] for the classic two-marginal OT setting, we derive gradient updates and efficient c -transform routines for such costs, to solve the MMOT problem. The pushforward map, as a part of the solution to the MMOT, is accurate and is used for the regularization-free applications, including the Wasserstein interpolation and the Wasserstein

barycenter.

The paper is organized as follows. In [section 2](#), we provide two parts of preliminaries. In the first part, we provide with all ingredients to understand the back-and-forth method (BFM). The concept of gradient in the Hilbert space is the key to BFM. In the second part, we introduce the MMOT problem with a focus on the duality theory, and basic graph theory for our description. In [section 3](#), we introduce the graphical representation of MMOT under assumptions (A1)–(A3), and transform any MMOT of such type of cost functions into an equivalent MMOT that has a tree representation, thanks to [Theorem 3.4](#). In [section 4](#), we introduce the main algorithm [Algorithm 1](#) to solve any MMOT that has a tree representation. We utilize [subsection 4.1](#) as a motivation and obtain the main algorithm for general cases in [subsection 4.2](#) and [subsection 4.3](#). In particular, we provide a detailed study on the Wasserstein barycenter in [subsection 4.4](#), as an important application of our methods. Numerical results for the comparison and validation with previous methods, a simple variant but a accelerator of [Algorithm 1](#), and a numerical result of the Wasserstein barycenter are presented in [section 5](#). We close this work with concluding thoughts in [section 6](#).

2. Preliminaries.

2.1. Two-Marginal Primal Formulation. The classic two-marginal OT problem is a resource allocation problem. Given two Borel probability measures μ_1, μ_2 on metric spaces X_1, X_2 and a continuous cost function $c : X_1 \times X_2 \rightarrow [0, +\infty]$, the classic Monge OT problem is to find the cheapest way to transport μ_1 to μ_2 :

$$(2.1) \quad \inf_T \left\{ \int c(x, T(x)) d\mu_1(x) : (T)_\# \mu_1 = \mu_2 \right\}.$$

The measures μ_1 and μ_2 are often referred as the *source measure* and the *target measure*, respectively. The *transport map* T satisfies the push-forward condition $(T)_\# \mu_1 = \mu_2$, which is shorthand notation for the condition that $\mu_2(A) = \mu_1(T^{-1}(A))$ for all Borel sets $A \subset X_2$. The optimal transport map T^* is called the *Monge map*. The Monge map does not always exist. For example, if μ_1 has fewer atoms than μ_2 , then mass from the same point in X_1 must be mapped to multiple points in X_2 , which cannot be accomplished by the deterministic map T . Kantorovich provided a relaxation of (2.1) that circumvents this issue. The Kantorovich problem takes the form

$$(2.2) \quad \inf \left\{ \int_{X_1 \times X_2} c(x_1, x_2) dP(x_1, x_2) : P \in \Gamma(\mu_1, \mu_2), \right\}$$

where $\Gamma(\mu_1, \mu_2)$ is the set of *transport plans* defined by

$$\Gamma(\mu_1, \mu_2) = \{P \in \mathbb{P}(X_1 \times X_2) : (\pi_1)_\# P = \mu_1, (\pi_2)_\# P = \mu_2\},$$

and π_1, π_2 are projection maps on each coordinate¹. The set of transport plans $\Gamma(\mu_1, \mu_2)$ consists of all joint probability measures on $X_1 \times X_2$ with marginals μ_1 and μ_2 . If no confusion

¹We distinguish between the projection of measures and the canonical projection of measures. For example, given a probability measure P on the space $(X_1 \times X_2) \times X_3 \cdots \times X_m$, then the projection of measures $(\pi_1)_\# P = P_1 \in \mathbb{P}(X_1), (\pi_2)_\# P = P_2 \in \mathbb{P}(X_2)$, while the canonical projection of measures $(\mathbf{Proj}_1)_\# P = P_{12} \in \mathbb{P}(X_1 \times X_2), (\mathbf{Proj}_2)_\# P = P_3 \in \mathbb{P}(X_3)$. This will be used in [Lemma 3.2](#).

may arise, we also use P_i as shorthand notation for $(\pi_i)_\#P$. When the source distribution μ_1 is atomless, the transport plan P^* solving the Kantorovich problem collapses onto the graph of the Monge solution and $P^* = (\text{id}, T^*)_\#\mu_1$, where $\text{id} : X_1 \rightarrow X_1$ is the identity map (see [Vil03]).

When $X_1 = X_2 = (X, d)$ and $c(x_1, x_2) = d^2(x_1, x_2)$ for some metric d , the minimal objective value in (2.2) defines a metric on the space of probability measures, called the (square of) *2-Wasserstein distances*, denoted by $W_2^2(\mu_1, \mu_2)$, which “lift” the metric d of space X to the space of probability measures on X . The solution of (2.2) also provides a natural way of interpolating between the source measure μ_1 and target measure μ_2 . The *displacement interpolation* in [McC01] is given by $\rho_t = (T_t)_\#P^*$, where $T_t(x_1, x_2) = (1-t)x_1 + tx_2$. When the Monge map T^* to (2.1) exists, the interpolation is given by $\rho_t = (\bar{T}_t)_\#\mu_0$ where $\bar{T}_t(\cdot) = (1-t)\text{id} + tT^*$. For both cases, we have $\rho_0 = \mu_1$ and $\rho_1 = \mu_2$.

2.2. Two-Marginal Duality Theory. Instead of solving (2.2) directly, it is often more efficient to solve the dual form of (2.2). From here on we will restrict our attention to spaces $X_1 = X_2 = \Omega \subset (\mathbb{R}^d, |\cdot|_2)$ that are convex and compact, as well as costs in the form $c(x_1, x_2) = h(x_1 - x_2)$ for a strictly convex function $h : \mathbb{R}^d \mapsto \mathbb{R}$. Furthermore, we assume all marginals (μ_i) are probability measures that are absolutely continuous with respect to the Lebesgue measure. Under these constraints, we have the following theorem

Theorem 2.1 ([San15], Theorem 1.40). *The dual problem to (2.2)*

$$(2.3) \quad \sup \left\{ \int_{X_1} f_1 d\mu_1 + \int_{X_2} f_2 d\mu_2 : f_1 \in L^1(\mu_1), f_2 \in L^1(\mu_2), f_1(x_1) + f_2(x_2) \leq c(x_1, x_2) \right\}$$

admits a c -conjugate solution (f_1^, f_2^*) . That is, $f_1^*(x_1) = \inf_{x_2} c(x_1, x_2) - f_2^*(x_2)$ and $f_2^*(x_2) = \inf_{x_1} c(x_1, x_2) - f_1^*(x_1)$. (See Definition 2.2.) Furthermore, strong duality between (2.2) and (2.3) holds.*

As a result of strong duality, the maximal objective value in the dual problem (2.3) is equal to the minimum objective in the primal problem (2.2). When the cost function is given by $c(x_1, x_2) = |x_1 - x_2|^2$, this implies the optimal value of the dual problem is the Wasserstein distance $W_2^2(\mu_1, \mu_2)$.

As discussed in [AG13], because the optimal dual variables satisfy $f_1^*(x_1) + f_2^*(x_2) = c(x_1, x_2)$ on the support of the optimal coupling P^* , the Monge map can be recovered from the optimal dual solution f_1^*, f_2^* when the map exists. See Lemma A.3 and Theorem A.4 in the supplementary document.

2.3. c -Transform. The constraint in (2.3) induces a key concept in computational OT: the c -transform. The c -transform is a natural generalization of the more common Legendre-Fenchel transform.

Definition 2.2 (Two-marginal c -transform). *The c -transform of a function $f : X_1 \mapsto \mathbb{R}$ is given by*

$$f^c(x_2) = \inf_{x_1} c(x_1, x_2) - f(x_1).$$

In addition, we say that f is c -concave if there exists a function $g : X_2 \mapsto \mathbb{R}$ such that $f = g^c$. We say (f_1, f_2) are c -conjugate if $f_1 = f_2^c$ and $f_2 = f_1^c$.

Remark 2.3. The c -transform cannot decrease the objective value in (2.3). For any feasible dual variables f_1 and f_2 , and any fixed point x_2 , we have $f_2(x_2) \leq c(x_1, x_2) - f_1(x_1)$ for all x_1 . This implies that $f_2(x_2) \leq f_1^c(x_2)$ and subsequently $\int_{X_2} f_2 d\mu_2 \leq \int_{X_2} f_1^c d\mu_2$.

Definition 2.4 (Legendre-Fenchel transform). *The Legendre-Fenchel transform of a function $\phi(x) : \mathbb{R}^d \mapsto \mathbb{R}$, denoted by $\phi^*(y)$, which is also called the convex conjugate, is given by*

$$\phi^*(y) = \sup_x x \cdot y - \phi(x).$$

Interested readers may refer to [Roc70] for convex analysis tools, or to [ABS21] for more connections between the Legendre transform and c -transform. We also put all necessary contents in the supplemental document.

Given $c(x_1, x_2) = h(x_1 - x_2)$ for some strictly convex function $h(\cdot) : \mathbb{R}^d \mapsto \mathbb{R}$, the map $S_f(x_1) \triangleq x_1 - \nabla h^*(\nabla f(x_1))$ will serve as a key ingredient in the classical OT theory. In particular, if $f = g^c$ for some continuous function g , then $S_f(x_1)$ is the unique minimizer to $\inf_{x_2} c(x_1, x_2) - g(x_2)$. Please refer to the supplemental document.

2.4. Gradient-based Optimization for OT. As a result of Remark 2.3 (also see Proposition 1.11 in [San15]), the dual problem is equivalent to either of the following problems

$$(2.4a) \quad \sup \left\{ I_1(f_1) = \int_{X_1} f_1 d\mu_1 + \int_{X_2} f_1^c d\mu_2 : f_1 \text{ is } c\text{-concave} \right\};$$

$$(2.4b) \quad \sup \left\{ I_2(f_2) = \int_{X_1} f_2^c d\mu_1 + \int_{X_2} f_2 d\mu_2 : f_2 \text{ is } c\text{-concave} \right\},$$

whose maximizers are guaranteed to exist. Concavity and existence of a c -concave maximizer was proved by Brenier [Bre91] for $c(x_1, x_2) = \frac{1}{2}|x_1 - x_2|^2$ and by Gangbo and McCann [GM96] for more general cost functions.

The concavity of (2.4a) and (2.4b) suggest that some form of gradient-based optimization could be effective at solving these problems. A gradient ascent step, for example, would take the form

$$(2.5) \quad f^{(k+1)} = f^{(k)} + \sigma \nabla I(f^{(k)}),$$

where $f^{(k)}$ is the value of the dual variable at optimization iteration k , $\sigma \in \mathbb{R}$ is a step size parameter, and $\nabla I(f^{(k)})$ is a functional gradient of I with respect to a dual variable f (i.e., f_1 in (2.4a) or f_2 in (2.4b)). The Fréchet derivatives provide a mechanism for defining the gradient in a suitable Hilbert space.

Definition 2.5 (Fréchet derivatives and gradient in the Hilbert space). *Given a separable Hilbert space $(\mathcal{H}, \|\cdot\|_{\mathcal{H}})$ and a functional $E : \mathcal{H} \mapsto \mathbb{R} \cup \{+\infty\}$, we say a bounded linear operator $\delta E_u : \mathcal{H} \mapsto \mathbb{R}$ is the Fréchet derivative of E at $u \in \mathcal{H}$ in the direction $v \in \mathcal{H}$ if*

$$\lim_{\|v\|_{\mathcal{H}} \rightarrow 0} \frac{|E(u+v) - E(u) - \delta E_u(v)|}{\|v\|_{\mathcal{H}}} = 0.$$

The gradient $\nabla_{\mathcal{H}}E(u) \in \mathcal{H}$ is then defined as an element in the Hilbert space that can be used to compute any directional Fréchet derivative through an inner product. More specifically, we say $\nabla_{\mathcal{H}}E(u)$ is the Hilbert space gradient of E at u if

$$\langle \nabla_{\mathcal{H}}E(u), v \rangle = \delta E_u(v), \quad \text{for all } v \in \mathcal{H}.$$

Note that the choice of Hilbert space defines the inner product and thus the form of the gradient. Jacobs and Léger [JL20] show that for $c(x_1, x_2) = \frac{1}{2}|x_1 - x_2|^2$, guaranteeing the ascent of (2.5) requires that the space \mathcal{H} cannot be weaker than

$$\dot{H}^1(\Omega) \triangleq \left\{ u : \Omega \mapsto \mathbb{R} : \int_{\Omega} u dx = 0, \int_{\Omega} |\nabla u(x)|^2 dx < \infty \right\},$$

with the inner product

$$\langle u_1, u_2 \rangle_{\dot{H}^1} = \int_{\Omega} \nabla u_1 \cdot \nabla u_2 dx.$$

For cost function $c(x_1, x_2) = h(x_1 - x_2)$ for some strictly convex function $h(\cdot) : \mathbb{R}^d \mapsto \mathbb{R}$, Lemma 3 in [JL20] shows that this choice of space and inner product results in the gradient:

$$(2.6) \quad \begin{aligned} \nabla_{\dot{H}^1} I_1(f_1) &= (-\Delta)^{-1} \left(\mu_1 - (S_{f_1^c})_{\#} \mu_2 \right); \\ \nabla_{\dot{H}^1} I_2(f_2) &= (-\Delta)^{-1} \left(\mu_2 - (S_{f_2^c})_{\#} \mu_1 \right), \end{aligned}$$

where $\Delta = \nabla \cdot \nabla$ is the Laplacian operator, and the pushforward map $S_f(x)$ is given by

$$(2.7) \quad S_f(x) \triangleq x - \nabla h^*(\nabla f(x)).$$

In fact, as shown by Brenier [Bre91] for the quadratic cost and by Gangbo and McCann for strictly convex costs, the maximizer (f_1, f_1^c) to (2.4a) (analogously with (f_2^c, f_2) to (2.4b)) induces mappings S_{f_1} and $S_{f_1^c}$ (analogously with S_{f_2} and $S_{f_2^c}$), which satisfy that

- $(S_{f_1})_{\#} \mu_1 = \mu_2$ and $(S_{f_1^c})_{\#} \mu_2 = \mu_1$;
- $S_{f_1} : X_1 \mapsto X_2$ defines the unique minimizer to $\inf_{x_2} c(x_1, x_2) - f_1^c(x_2)$; and $S_{f_1^c} : X_2 \mapsto X_1$ defines the unique minimizer to $\inf_{x_1} c(x_1, x_2) - f_1(x_1)$.

In this sense, formulas (2.6) are natural, as one may observe that $\mu_1 = (S_{f_1^c})_{\#} \mu_2$ corresponds to the gradient being zero $\nabla_{\dot{H}^1} I_1(f_1) = 0 \in \dot{H}^1$ and the inverse Laplacian $(-\Delta)^{-1}$ stems from the inner product structure of the Hilbert space \dot{H}^1 .

2.5. Multi-Marginal Primal Formulation. A natural extension of the two-marginal problem in (2.2) is to the multi-marginal problem, given by

$$(2.8) \quad \inf_{P \in \Gamma(\mu_1, \dots, \mu_m)} \int c(x_1, \dots, x_m) dP(x_1, \dots, x_m),$$

for the space $\mathbf{X} = X_1 \times \dots \times X_m$ and prescribed marginal probability measures $(\mu_i)_{i=1}^m$, the set of transport plans $\Gamma(\mu_1, \dots, \mu_m)$ is defined by

$$\Gamma(\mu_1, \dots, \mu_m) \triangleq \{ P \in \mathbb{P}(\mathbf{X}) \mid (\pi_i)_{\#} P = \mu_i, 1 \leq i \leq m \}.$$

That is, $P(X_1 \times \cdots \times A_i \times \cdots \times X_m) = \mu_i(A_i)$ for all measurable sets $A_i \subset X_i$ and any $i \in \{1, 2, \dots, m\}$. For notational simplicity, we will also denote the constraint by $P_i = \mu_i$ when the intent is clear. Analogously, the joint marginal $P_{ij} \triangleq (\pi_{ij})_{\#} P$ satisfies $\int_{X_1 \times \cdots \times A_i \times \cdots \times A_j \times \cdots \times X_m} dP = \int_{A_i \times A_j} dP_{ij}$ for all Borel sets $A_i \subset X_i$ and $A_j \subset X_j$.

Applications of MMOT vary in the type of cost function used. In density functional theory, costs of the form $c(x_1, \dots, x_m) = \sum_{i < j} |x_i - x_j|^{-1}$ or $c(x_1, \dots, x_m) = \sum_{i < j} -\log(|x_i - x_j|)$ arise (see [DMGN17]). Applications in minimal action interpolation use $c(x_1, \dots, x_m) = \sum_{i=1}^{m-1} \tau^{-1} |x_i - x_{i+1}|^2$ (see [Bre89]). Wasserstein barycenters can be formulated as MMOTs with costs of the form $c(x_1, \dots, x_m) = \sum_{1 \leq i < j \leq m} \lambda_i \lambda_j |x_i - x_j|^2$ (see [GS98, AC11], also see subsection 4.4). An important feature of these costs is that they are all defined pairwise and fall in the same family of pairwise costs with the form

$$c(x_1, \dots, x_m) = \sum_{1 \leq i < j \leq m} c_{ij}(x_i, x_j).$$

Due to their broad applicability, such pairwise costs will be the focus of this work.

2.6. Multi-Marginal Duality Theory. Assume the cost function $c(x_1, \dots, x_m)$ is continuous and each μ_i is supported on a convex and compact subset in \mathbb{R}^d . The dual problem corresponding to (2.8) is given by

$$(2.9) \quad \sup_{(f_1, \dots, f_m)} \sum_{i=1}^m \int_{X_i} f_i(x_i) d\mu_i,$$

where $f_i \in L^1(\mu_i)$ and $\sum_{i=1}^m \int_{X_i} f_i(x_i) d\mu_i \leq c(x_1, \dots, x_m)$. We call the optimal tuple (f_1, \dots, f_m) as the *Kantorovich potentials*.

The concept of a c -splitting set extends the notion of a c -transform to the multi-marginal setting. A set $G \subset \mathbf{X}$ is a c -splitting set, if there exist m functions $f_i : X_i \mapsto [-\infty, \infty)$ such that

$$\begin{cases} \sum_{i=1}^m f_i(x_i) \leq c(x_1, x_2, \dots, x_m) & \text{on } X; \\ \sum_{i=1}^m f_i(x_i) = c(x_1, x_2, \dots, x_m) & \text{in } G. \end{cases}$$

These functions (f_1, f_2, \dots, f_m) are called a c -splitting tuple.

Much like the c -transform was guaranteed to not decrease the dual objective in the two-marginal setting, for a c -splitting tuple (f_1, \dots, f_m) , there exists a c -conjugate tuple $(\tilde{f}_1, \dots, \tilde{f}_m)$, that is, for any i ,

$$\tilde{f}_i(x) = \left(\sum_{j \neq i} \tilde{f}_j \right)^c \triangleq \inf_{\text{all } y_j} c(y_1, \dots, y_{i-1}, x, y_{i+1}, \dots, y_m) - \sum_{j \neq i} \tilde{f}_j(y_j),$$

which is always a better candidate to (2.9). This is due to the fact that $f_i(x_i) \leq \tilde{f}_i(x_i)$ for any $x_i \in X_i$. The c -conjugate tuple $(\tilde{f}_1, \tilde{f}_2, \dots, \tilde{f}_m)$ can be constructed from:

$$\begin{cases} \tilde{f}_1(x) = \inf_{\text{all } y_j} c(x, y_2, \dots, y_m) - \sum_{j \geq 2} f_j(y_j); \\ \tilde{f}_i(x) = \inf_{\text{all } y_j} c(y_1, \dots, y_{i-1}, x, y_{i+1}, \dots, y_m) - \sum_{j < i} \tilde{f}_j(y_j) - \sum_{j > i} f_j(y_j). \end{cases}$$

This is called a ‘‘convexification trick’’ in the context of convex analysis [CN08].

The existence of optimal solutions to (2.8) and (2.9), and the strong duality between these problems, was proved by [Kel84] for more general non-pairwise cost functions. When $X_i = \mathbb{R}^d$, [CN08] also showed the existence of a c -conjugate optimal solution to (2.9) for general continuous cost functions. An extension of this result by [Pas11] provides an explicit connection between the primal and dual MMOT problems. Let $(\tilde{f}_1, \dots, \tilde{f}_m)$ be a c -conjugate solution to the dual problem (2.9) and let P be the optimal transport plan to primal problem in (2.8), then we have the following connection between the primal solution and dual solution

$$\sum_{i=1}^m \tilde{f}_i(x_i) = c(x_1, \dots, x_m) \quad P\text{-a.e.}$$

[Pas11] also showed that when the cost $c(x_1, \dots, x_m)$ is continuously differentiable and each marginal μ_i has a strictly positive density, the solution to (2.9) is unique up to constant. That is, $(\tilde{f}_1 + a_1, \tilde{f}_2 + a_2, \dots, \tilde{f}_m + a_m)$ is also a solution, provided with $\sum_{i=1}^m a_i = 0$.

2.7. Graph Theory. A graph $G = (V, E)$ is described by a set of nodes V and set of edges E . We will consider graphs where each node is associated with a marginal distribution μ_i , or with a dual variable f_i , and will simply use the index i to denote the node. An edge $e = (s, t) \in E$ from node s to t will then represent the pairwise cost $c_{st}(x_s, x_t)$. We will restrict our attention to *simple graphs*, which do not contain self-loops or multiple edges.

We will use both *directed* (where the order of the edge (s, t) matters) and *undirected graphs* (where edges are order-agnostic). For directed graphs, we will use $N^+(i) = \{e_t : e \in E \text{ and } e_s = i\}$ and $N^-(i) = \{e_s : e \in E \text{ and } e_t = i\}$ to denote the sets of downstream nodes and upstream nodes neighboring node i , respectively. A particular type of graph called a *tree* will also be important to our approach. A tree is a graph where any two nodes are only connected by a single path. A *rooted tree* is a tree graph where all of the edges flow towards a single node, called the root. In a rooted tree with edges pointing towards root node r , the cardinality of the downstream set $|N^+(i)| = 1$ for $i \neq r$ and $|N^+(r)| = 0$.

3. Graphical Representation of MMOT. In section 4 we will introduce a novel computational approach to solving MMOT problems with pairwise costs. A key component of that approach is the graphical representation of pairwise MMOT problems established below.² This section also establishes one of our main theoretical results in **Theorem 3.4**: that any MMOT

²We adopt the terminology that the MMOT problem itself admits a graph structure, rather than saying that the **cost function** has a graph structure, which is the terminology used in [HSZ⁺21, HRCK21]. This distinction is prevent confusion with the branched optimal transport problem (see e.g., [Xia03, MSM03, BCM08]).

problem with pairwise cost can be represented as a rooted tree with nodes corresponding to marginal distributions and edges corresponding to pairwise costs.

While the duality theory described above in [subsection 2.6](#) holds in more general settings, the rest of this paper will consider cost functions that satisfy the following three assumptions:

(A1) The cost function can be expressed as a sum of pairwise costs:

$$c(x_1, \dots, x_m) = \sum_{1 \leq i < j \leq m} c_{ij}(x_i, x_j);$$

(A2) At least $m - 1$ functions $c_{ij}(x_i, x_j)$ are not identically zero;

(A3) For each pair (i, j) , $c_{ij}(x_i, x_j) = h_{ij}(x_i - x_j)$ for some strictly convex function h_{ij} .

The pairwise assumption (A1) causes the cost function to have a graph structure. The assumption (A2) ensures that the MMOT cannot be divided into multiple independent MMOT problems. Note that problems that do not satisfy the assumption (A2) can be trivially split into subproblems that do satisfy this assumption. The assumption (A3) enables a concise representation of the pushforward map (see discussions in [subsection 2.4](#) or [Theorem A.4](#) in the supplemental document) and enables computationally efficient evaluations of c_{ij} -transforms. As a result of the general duality theory established by [Kel84], under (A1)–(A3) the primal and dual MMOT problems in (2.8) and (2.9) both admit solutions, and strong duality holds.

The MMOT problem (2.8) under assumption (A1) is analogous to an undirected graph with m nodes representing the marginals, and with edges for all costs $c_{st}(x_s, x_t)$ that are not identically 0. This bijection is illustrated in [Figure 1](#) for several MMOT problems.

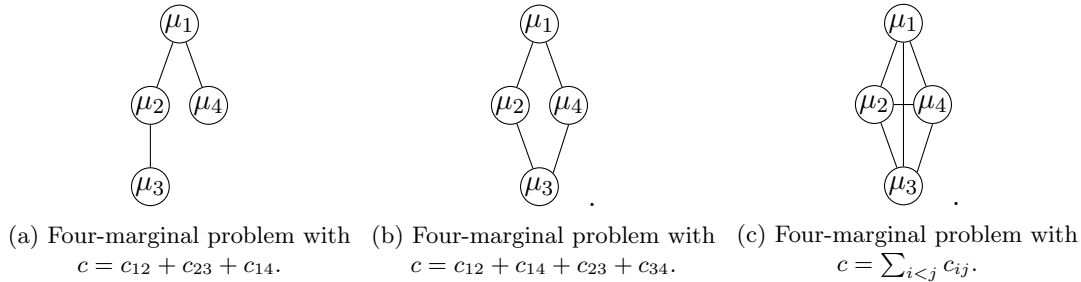


Figure 1: Undirected Graphical representations of MMOT problems with $m = 4$ marginals. (a) shows a cost that can be represented directly as a tree, whereas (b) and (c) are cyclic graphs. [Theorem 3.4](#) provides a mechanism for unrolling these cyclic graphs in equivalent MMOT problems with tree structures. Also note that (c) shows the structure that arises in the MMOT formulation of Wasserstein barycenter problems (see [subsection 4.4](#)).

As we show below in [section 4](#), MMOT problems that admit tree representations, like [Figure 1a](#), can be efficiently solved with a gradient-based optimization strategy generalized from the back-and-forth method of [JL20] for two-marginal OT problems. In [Theorem 3.4](#) below, we show that the solution of MMOT problems without this tree structure (e.g., [Figure 1b](#) and [Figure 1c](#)) can be obtained through the solution of a larger "unrolled" problem that does exhibit this tree structure. This fundamental result therefore allows us to apply our tree-based approach to any MMOT problem with pairwise costs.

The following lemma establishes a connection between the size of an MMOT problem with cyclic graph and the size of an equivalent problem with a tree structure.

Lemma 3.1. *Given an undirected graph $G = (V, E)$ with possible cycles, we need exactly $|E| + 1 - |V|$ duplicate nodes to be unrolled into a tree.*

Proof. Adding duplicate nodes and replacing original edges, the new graph retains the same number of edges while becoming a tree. A tree of $|E|$ edges has $|E| + 1$ nodes. Thus we need to add $|E| + 1 - |V|$ duplicate nodes. \blacksquare

To show that solving any pairwise MMOT is equivalent to solving another MMOT with a tree representation, we will need the following generalized gluing lemma.

Lemma 3.2 (Generalized gluing lemma, Theorem A.1 in [dA82]). *Let J be an arbitrary index set and for each $j \in J$, let X_j, Y_j be Polish spaces and $\mathbf{X} = \prod_{j \in J} X_j, \mathbf{Y} = \prod_{j \in J} Y_j$. Let $\phi_j : X_j \mapsto Y_j$ be a measurable map and let $\mu_j \in \mathbb{P}(X_j)$. Let $Q \in \mathbb{P}(\mathbf{Y})$ such that $(\phi_j)_\# \mu_j = (\mathbf{Proj}_j)_\# Q$ for all $j \in J$.*

Then there exists a $P \in \mathbb{P}(\mathbf{X})$ such that:

$$\begin{cases} (\mathbf{Proj}_j)_\# P = \mu_j, & \text{for all } j \in J; \\ \left(\left(\phi_j \circ \mathbf{Proj}_j \right)_{j \in J} \right)_\# P = Q. \end{cases}$$

Remark 3.3. As pointed out in the bibliographic comments of Dudley [Dud99], the assumption of Polish spaces can be weakened to be any Borel sets in Polish spaces.

We are now ready to show that any pairwise MMOT problem can be “unrolled” into an equivalent MMOT problem with a tree structure. Qualitatively, the process of unrolling a graph is illustrated in Figure 2, where a single cycle is broken by duplicating the marginal μ_4 . This process is made more precise in Theorem 3.4.

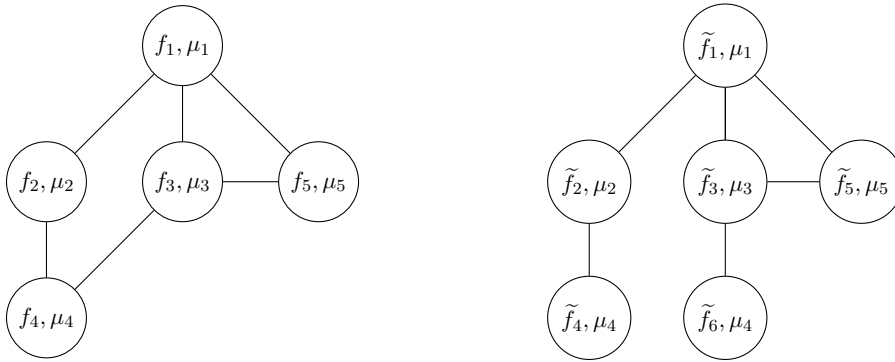


Figure 2: Breaking one cycle in the left graph with m nodes results in the right graph with $m + 1$ nodes. Theorem 3.4 repeats this process to obtain a tree and convert any pairwise MMOT problem into an equivalent problem with a tree structure.

Theorem 3.4. *Given a cost function $c(x_1, \dots, x_m)$ satisfying assumptions (A1), (A2) and (A3) that corresponds to an undirected graph $G = (V, E)$ with possible cycles, there exists a cost function $\bar{c}(x_1, \dots, x_n)$ that corresponds to another undirected tree $\bar{G} = (\bar{V}, \bar{E})$ with $n = |\bar{V}| = |E| + 1$ nodes, such that*

$$\inf_{P^{(m)} \in \Gamma(\mu_1, \dots, \mu_m)} \int c(x_1, \dots, x_m) dP^{(m)} = \inf_{P^{(n)} \in \Gamma(\mu_1, \dots, \mu_n)} \int \bar{c}(x_1, \dots, x_n) dP^{(n)},$$

where $(\mu_k)_{k=m+1}^n$ are duplicated from $(\mu_i)_{i=1}^m$ in the “unrolling” process.

Furthermore, let $P^{(m)}$ and $(f_i)_{i=1}^m$ be the optimal primal and dual solutions to the original MMOT, such that

$$\int c(x_1, \dots, x_m) dP^{(m)} = \sum_{i=1}^m \int f_i(x_i) d\mu_i.$$

And $P^{(n)}$ and $(\bar{f}_i)_{i=1}^n$ be the optimal primal and dual solutions to the new MMOT, such that

$$\int \bar{c}(x_1, \dots, x_n) dP^{(n)} = \sum_{i=1}^n \int \bar{f}_i(x_i) d\mu_i,$$

then for any i , the original dual variable f_i is the sum of all \bar{f}_j whose nodes are duplicated from μ_i .

Proof. We prove it by iteration. Assume there is a cycle in $G = (V, E)$ and we can remove an edge $e = (i, j)$ to break the cycle. Let $c(x_1, \dots, x_m) = c_{ij}(x_i, x_j) + d(x_1, \dots, x_m)$ and $\tilde{c}(x_1, \dots, x_{m+1}) = c_{ij}(x_i, x_{m+1}) + d(x_1, \dots, x_m)$. By defining a map: $T : X_1 \times \dots \times X_m \mapsto X_1 \times \dots \times X_m \times X_j$ given by $T(x_1, \dots, x_j, \dots, x_m) = (x_1, \dots, x_j, \dots, x_m, x_j)$, we note that: $c = \tilde{c} \circ T$, thus for any $P \in \mathbb{P}(X_1 \times \dots \times X_m)$, we have

$$(3.1) \quad \int c(x_1, \dots, x_m) dP = \int \tilde{c} \circ T dP = \int \tilde{c} d[(T)_\# P].$$

Consider the following two subsets $\mathcal{Q}_1, \mathcal{Q}_2$ of couplings in $\mathbb{P}(X_1 \times \dots \times X_m \times X_j)$, where

$$\begin{aligned} \mathcal{Q}_1 &= \{Q \in \mathbb{P}(X_1 \times \dots \times X_m \times X_j) \mid Q_i = \mu_i \text{ for all } i \notin \{j, m+1\}; Q_{j, m+1} = ((\text{id}, \text{id}))_\# \mu_j\}, \\ \mathcal{Q}_2 &= \{Q = (T)_\# P \in \mathbb{P}(X_1 \times \dots \times X_m \times X_j) \mid P \in \Gamma(\mu_1, \dots, \mu_m)\}. \end{aligned}$$

We first show that these two sets are equivalent.

For a coupling $Q \in \mathcal{Q}_2$, when $i \notin \{j, m+1\}$ and for any Borel sets A_i in X_i , we have

$$Q_i(A_i) = (\pi_i)_\# Q(A_i) = (\pi_i)_\# ((T)_\# P)(A_i) = P(T^{-1} \circ \pi_i^{-1}(A_i)) = \mu_i(A_i).$$

Also, for any Borel sets $A_j \subset X_j$ and $A_{m+1} \subset X_{m+1}$:

$$\begin{aligned} Q_{j, m+1}(A_j \times A_{m+1}) &= ((\pi_j, \pi_{m+1}))_\# Q(A_j \times A_{m+1}) = P(T^{-1} \circ (\pi_j, \pi_{m+1})^{-1}(A_j \times A_{m+1})) \\ &= P(T^{-1}(X_1 \times \dots \times A_j \times X_{j+1} \times \dots \times X_m \times A_{m+1})) \end{aligned}$$

$$\begin{aligned}
&= P(X_1 \times \cdots \times (A_j \cap A_{m+1}) \times \cdots \times X_m) \\
&= \mu_j(A_j \cap A_{m+1}) = ((\text{id}, \text{id}))_{\#} \mu_j(A_j \times A_{m+1}).
\end{aligned}$$

Thus $Q \in \mathcal{Q}_1$, showing that $\mathcal{Q}_2 \subseteq \mathcal{Q}_1$.

On the other hand, consider a coupling $Q \in \mathcal{Q}_1$. Comparing with [Lemma 3.2](#), we have (X_i, μ_i) , take $Y_i = X_i$ for $i \neq j$ and $Y_j = X_j \times X_{m+1}$ with $X_{m+1} = X_j$, thus $\mathbf{Y} = X_1 \times \cdots \times (X_j \times X_{m+1}) \times \cdots \times X_m$. For $i \neq j$, define $\phi_i = \text{id} : X_i \mapsto Y_i$ and $\phi_j : X_j \mapsto Y_j$ by $\phi_j = (\text{id}, \text{id})$. Up to a permutation, we treat $Q \in \mathbb{P}(X_1 \times \cdots \times X_m \times X_j)$ as $Q \in \mathbb{P}(\mathbf{Y})$, thus by the definition of \mathcal{Q}_1 , we have:

$$(\phi_i)_{\#} \mu_i = (\mathbf{Proj}_i)_{\#} Q; \quad \text{and} \quad ((\text{id}, \text{id}))_{\#} \mu_j = (\mathbf{Proj}_j)_{\#} Q$$

Thanks to [Lemma 3.2](#), there exists a $P \in \mathbb{P}(\mathbf{X})$ such that:

$$\begin{cases} (\mathbf{Proj}_i)_{\#} P = \mu_i & \text{for all } i; \\ ((\phi_1 \circ \mathbf{Proj}_1, \cdots, \phi_j \circ \mathbf{Proj}_j, \cdots, \phi_m \circ \mathbf{Proj}_m))_{\#} P = Q. \end{cases}$$

Note that

$$\begin{aligned}
&(\phi_1 \circ \mathbf{Proj}_1, \cdots, \phi_j \circ \mathbf{Proj}_j, \cdots, \phi_m \circ \mathbf{Proj}_m)(x_1, \cdots, x_j, \cdots, x_m) \\
&= (\phi_1(x_1), \cdots, \phi_j(x_j), \cdots, \phi_m(x_m)) = (x_1, \cdots, (x_j, x_j), \cdots, x_m),
\end{aligned}$$

which is a permutation of T . As we prove the existence of $P \in \Gamma(\mu_1, \cdots, \mu_m)$, thus $Q \in \mathcal{Q}_2$ and subsequently $\mathcal{Q}_1 \subseteq \mathcal{Q}_2$. Combined with the discussion above, this implies that $\mathcal{Q}_1 = \mathcal{Q}_2$.

Using this equivalence and [\(3.1\)](#) results in

$$\inf_{P \in \Gamma(\mu_1, \cdots, \mu_m)} \int c(x_1, \cdots, x_m) dP = \inf_{Q \in \mathcal{Q}_2} \int \tilde{c}(x_1, \cdots, x_{m+1}) dQ = \inf_{Q \in \mathcal{Q}_1} \int \tilde{c}(x_1, \cdots, x_{m+1}) dQ.$$

On one hand, by [subsection 2.6](#) we have the strong duality for the original MMOT:

$$(3.2) \quad \inf_{P \in \Gamma(\mu_1, \cdots, \mu_m)} \int c(x_1, \cdots, x_m) dP = \sup_{f_1 + \cdots + f_m \leq c} \sum_{i=1}^m \int f_i(x_i) d\mu_i,$$

on the other hand, we also have the strong duality for the new MMOT:

$$(3.3) \quad \inf_{P \in \Gamma(\mu_1, \cdots, \mu_m, \mu_{m+1})} \int \tilde{c}(x_1, \cdots, x_{m+1}) dQ = \sup_{\tilde{f}_1 + \cdots + \tilde{f}_{m+1} \leq \tilde{c}} \sum_{i=1}^{m+1} \int \tilde{f}_i(x_i) d\mu_i,$$

Once we prove the equivalence between these MMOTs in terms of primal problems, it follows with the equivalence in terms of dual problems, and the recovery from dual solutions to the new MMOT to dual solutions to the original MMOT.

Let $\mu_{m+1} = \mu_j$, among all bounded and continuous functions $(\tilde{f}_i)_{i=1}^{m+1}$, we have that

$$\begin{aligned}
& \sup \sum_{i=1}^{m+1} \int_{X_i} \tilde{f}_i d\mu_i - \int_{X_1 \times \cdots \times X_m \times X_j} \left(\sum_{i=1}^m \tilde{f}_i(x_i) \right) dQ \\
(3.4) \quad &= \sup \sum_{i \notin \{j, m+1\}} \int_{X_i} \tilde{f}_i d\mu_i - \int_{X_1 \times \cdots \times X_m \times X_j} \left(\sum_{i \notin \{j, m+1\}} \tilde{f}_i(x_i) \right) dQ + \\
& \quad + \int_{X_j} (\tilde{f}_j(x_j) + \tilde{f}_{m+1}(x_j)) d\mu_j - \int_{X_1 \times \cdots \times X_m \times X_j} (\tilde{f}_j(x_j) + \tilde{f}_{m+1}(x_{m+1})) dQ \\
&= \begin{cases} 0, & Q \in \mathcal{Q}_1; \\ +\infty, & Q \in \mathcal{M}_+(X_1 \times \cdots \times X_m \times X_j) \setminus \mathcal{Q}_1, \end{cases}
\end{aligned}$$

where $\mathcal{M}_+(X)$ is the space of positive finite measures. Thus by (3.4) and (3.3), we have

$$\begin{aligned}
(3.5) \quad & \inf_{P \in \Gamma(\mu_1, \dots, \mu_m)} \int c(x_1, \dots, x_m) dP = \inf_{Q \in \mathcal{Q}_1} \int \tilde{c}(x_1, \dots, x_{m+1}) dQ \\
&= \sup_{\tilde{f}_1 + \cdots + \tilde{f}_{m+1} \leq \tilde{c}} \sum_{i=1}^{m+1} \int_{X_i} \tilde{f}_i d\mu_i \\
&= \inf_{Q \in \Gamma(\mu_1, \dots, \mu_m, \mu_j)} \int \tilde{c}(x_1, \dots, x_{m+1}) dQ,
\end{aligned}$$

which sets up the equivalence between the original MMOT and the new MMOT.

Furthermore, let $(f_i)_{i=1}^m$ and $(\tilde{f}_i)_{i=1}^{m+1}$ be the Kantorovich potentials. Due to (3.5), (3.2) and (3.3), we have

$$\sum_{i=1}^m \int_{X_i} f_i d\mu_i = \sum_{i=1}^{m+1} \int_{X_i} \tilde{f}_i d\mu_i = \sum_{i \notin \{j, m+1\}} \int_{X_i} \tilde{f}_i d\mu_i + \int_{X_j} (\tilde{f}_j(x_j) + \tilde{f}_{m+1}(x_j)) d\mu_j.$$

Therefore we can define an optimal dual solution $(f_i)_{i=1}^m$ to the original problem, in terms of the optimal dual solution to the new problem:

$$\begin{cases} f_i = \tilde{f}_i, & i \neq j; \\ f_j = \tilde{f}_j + \tilde{f}_{m+1} & i = j. \end{cases}$$

The above process can be repeated to remove all cycles in the tree. [Lemma 3.1](#) guarantees that only a finite number of repetitions are required, thus completing the proof. ■

Remark 3.5. As we only use the duality theory between the Kantorovich problem and the dual problem in the proof, the theorem still holds if one drops assumption [\(A3\)](#) but adds some continuity assumption.

4. Computational Approach. To solve the MMOT problem, we need to maximize the dual functional

$$(4.1) \quad I(f_1, \dots, f_m) = \sum_{i=1}^m \int f_i d\mu_i$$

among dual variables satisfying $\sum_{i=1}^m f_i(x_i) \leq c(x_1, \dots, x_m)$. Similar to the two-marginal approach of [JL20], by leveraging c -transform to get rid of the constraint, we will use gradient ascent on the remaining $(m-1)$ dual variables in the space \dot{H}^1 . As shown below, the graphical interpretation of the MMOT problem will enable fast c -transforms and gradient updates in the multi-marginal setting.

On a high level, our algorithm consists of three steps:

- I) We first construct an undirected graph based on the cost function. This graph may have cycles.
- II) We follow [Theorem 3.4](#) and “unroll” the cyclic graph into an undirected tree, at the cost of adding duplicate nodes.
- III) We solve the unrolled problem by doing gradient ascent procedure described below in [section 4](#), following the orientation and layers of the tree.

We have discussed Step I and II in [section 3](#). As illustrated in [Figure 3](#), by picking arbitrary node as the root node, and traversing the undirected tree with a breadth first search to add directionality, we obtain a directed rooted tree. The main computational cost of our algorithm is in finding the solution to the MMOT problem that has a rooted tree representation.

4.1. Illustrative Example. To motivate our general gradient ascent approach, first consider a simple MMOT problem with three marginals μ_1, μ_2, μ_3 and cost

$$c(x_1, x_2, x_3) = c_{12}(x_1, x_2) + c_{23}(x_2, x_3).$$

We will need to derive gradients of the dual objective ((4.1) with $m = 3$) with respect to dual variables. For this particular example, it can be accomplished by making an analogy between the MMOT problem and multiple two-marginal OT problems. Due to the gluing lemma, the primal MMOT problem under this cost is analogous to the sum of two OT problems:

$$\inf_{P \in \Gamma(\mu_1, \mu_2, \mu_3)} \int c(x_1, x_2, x_3) dP = \inf_{P_{12} \in \Gamma(\mu_1, \mu_2)} \int c_{12}(x_1, x_2) dP_{12} + \inf_{P_{23} \in \Gamma(\mu_2, \mu_3)} \int c_{23}(x_2, x_3) dP_{23}.$$

The corresponding dual problem of the MMOT is

$$\begin{aligned} & \sup_{f_1, f_2, f_3} \int f_1(x_1) d\mu_1 + \int f_2(x_2) d\mu_2 + \int f_3(x_3) d\mu_3, \\ & \text{s.t. } f_1(x_1) + f_2(x_2) + f_3(x_3) \leq c(x_1, x_2, x_3), \end{aligned}$$

and the dual problem for the summed two-marginal problems is

$$\begin{aligned} & \sup_{u_1, v_1} \left[\int u_1(x_1) d\mu_1 + \int v_1(x_2) d\mu_2 \right] + \sup_{u_2, v_2} \left[\int v_2(x_2) d\mu_2 + \int u_2(x_3) d\mu_3 \right], \\ & \text{s.t. } u_1(x_1) + v_1(x_2) \leq c_{12}(x_1, x_2); \\ & \quad u_2(x_3) + v_2(x_2) \leq c_{23}(x_2, x_3), \end{aligned}$$

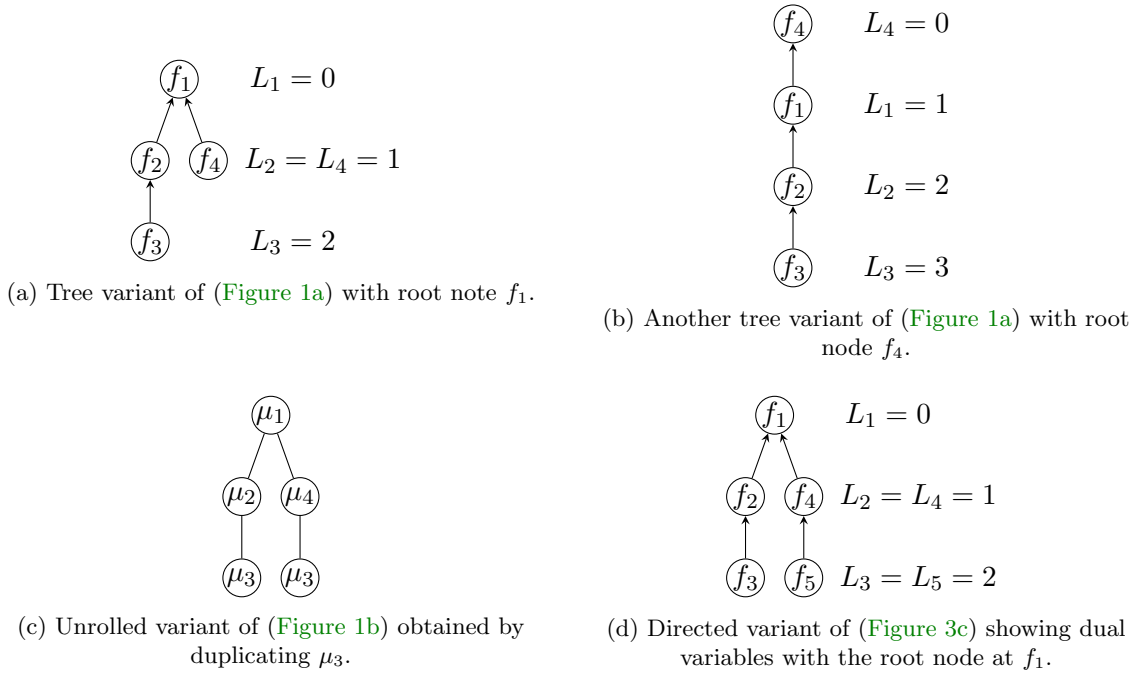


Figure 3: Directed tree representations of MMOTs with $m = 4$ marginals. We reserve dual variables (f_i) for nodes in directed trees. The first row is two possible directed tree representations of cost in Figure 1a. These are constructed by selecting a particular root node (either f_1 or f_4 in these examples) and then traversing the graph with a breadth first search to add directionality to each edge. The second row demonstrates how our algorithm works from Figure 1b. The layer L_i of node i is needed to provide an ordering in Algorithm 1.

where u_1, v_1 are loading/unloading prices for the OT problem under cost c_{12} and u_2, v_2 are loading/unloading prices for the OT problem under cost c_{23} .

4.1.1. Using $f_2 = (f_1 + f_3)^c$. In both dual problems, the constraints can be accounted for by using c -transforms to define one dual variable in terms of the others. Assume $f_2(x_2) = (f_1 + f_3)^c(x_2)$, $v_1(x_2) = u_1^{c_{12}}(x_2)$, and $v_2(x_2) = u_2^{c_{23}}(x_2)$, then the dual MMOT problem is

$$\sup_{f_1, f_3} \int f_1(x_1) d\mu_1 + \int (f_1 + f_3)^c(x_2) d\mu_2 + \int f_3(x_3) d\mu_3,$$

and the combined two-marginal dual problems become

$$(4.2) \quad \sup_{u_1} \left[\int u_1(x_1) d\mu_1 + \int u_1^{c_{12}}(x_2) d\mu_2 \right] + \sup_{u_2} \left[\int u_2^{c_{23}}(x_2) d\mu_2 + \int u_2(x_3) d\mu_3 \right].$$

These two expressions have exactly the same form because the pairwise structure of the cost yields $(f_1 + f_2)^c(x_2) = f_1^{c_{12}}(x_2) + f_3^{c_{23}}(x_2)$, which implies that

$$(4.3) \quad \sup_{f_1, f_3} \int f_1(x_1) d\mu_1 + \int f_1^{c_{12}}(x_2) d\mu_2 + \int f_3^{c_{23}}(x_2) d\mu_2 + \int f_3(x_3) d\mu_3.$$

Importantly, this implies that the two-marginal ascent directions in (2.6) can be adapted to define ascent directions for f_1 and f_2 in (4.3). In particular, let $I_2(f_1, f_3) = \int f_1 d\mu_1 + \int (f_1 + f_3)^c d\mu_2 + \int f_3 d\mu_3$ denote the dual MMOT objective with f_2 defined through the c -transform. Then the gradients take the form

$$(4.4) \quad \begin{aligned} \nabla_{\dot{H}^1} I_2(f_1; f_3) &= (-\Delta)^{-1}(\mu_1 - (S_{f_1^{c_{12}}})_{\#}\mu_2); \\ \nabla_{\dot{H}^1} I_2(f_3; f_1) &= (-\Delta)^{-1}(\mu_3 - (S_{f_3^{c_{23}}})_{\#}\mu_2). \end{aligned}$$

The identical relationship between (4.3) and (4.2) relied on the separable property $(f_1 + f_2)^c(x_2) = f_1^{c_{12}}(x_2) + f_3^{c_{23}}(x_2)$. Using the graphical interpretation of MMOT developed in section 3, we will later show that this corresponds to the fact that root node f_2 is the c -transform of leaf nodes f_1 and f_3 in a rooted tree, as shown in Figure 4b. A general situation is shown in Lemma 4.1.

4.1.2. Using $f_3 = (f_1 + f_2)^c$. More care is needed to make an analogy between the MMOT problem and two-marginal problems for orderings of the c -transform. For example, consider the dual problem when f_3 is defined through the c -transform of $f_1 + f_2$. In this case, the dual objective $I_3(f_1, f_2)$ takes the form

$$\sup_{f_1, f_2} \int f_1(x_1) d\mu_1 + \int f_2(x_2) d\mu_2 + \int (f_1 + f_2)^c(x_3) d\mu_3.$$

Expanding the c -transform is more difficult

$$(4.5) \quad \begin{aligned} (f_1 + f_2)^c(x_3) &= \inf_{x_1, x_2} c_{12}(x_1, x_2) + c_{23}(x_2, x_3) - f_1(x_1) - f_2(x_2) \\ &= \inf_{x_2} c_{23}(x_2, x_3) - f_2(x_2) + f_1^{c_{12}}(x_2) \\ &= (f_2 - f_1^{c_{12}})^{c_{23}}(x_3), \end{aligned}$$

but still results in a form that can be compared with (4.2)

$$\begin{aligned} &\sup_{f_1, f_2} \int f_1(x_1) d\mu_1 + \int f_2(x_2) d\mu_2 + \int (f_2 - f_1^{c_{12}})^{c_{23}}(x_3) d\mu_3 \\ &= \sup_{f_1, f_2} \int f_1(x_1) d\mu_1 + \int f_1^{c_{12}}(x_2) d\mu_2 + \int (f_2 - f_1^{c_{12}}) d\mu_2 + \int (f_2 - f_1^{c_{12}})^{c_{23}} d\mu_3. \end{aligned}$$

Using the same analogy with (2.6) as above, the gradients of I_3 take the form

$$(4.6a) \quad \nabla_{\dot{H}^1} I_3(f_1; f_2) = (-\Delta)^{-1}(\mu_1 - (S_{f_1'})_{\#}\mu_2);$$

$$(4.6b) \quad \nabla_{\dot{H}^1} I_3(f_2; f_1) = (-\Delta)^{-1}(\mu_2 - (S_{f_2'})_{\#}\mu_3),$$

where $f_1' = (f_1)^{c_{12}}$, $f_2' = (f_2 - f_1^{c_{12}})^{c_{23}}$ and $S_f(x)$ is defined in (2.7). These identities are made more rigorous in Lemma B.1 in the supplementary document.

The need to include $f_1^{c_{12}}$ in the definition of f_2' stems from the fact that there is no direct pairwise cost relating x_1 and x_3 . Here, the dual variable f_3 and f_1 are therefore only indirectly coupled through f_2 , which is illustrated in Figure 4c. This is in contrast to subsection 4.1.1, where the root node f_2 was directly coupled with f_1 and f_3 . As we will show in (4.8) below, expressions similar to f_2' can be used to propagate information through pairwise MMOT problems with an arbitrary number of marginal distributions.

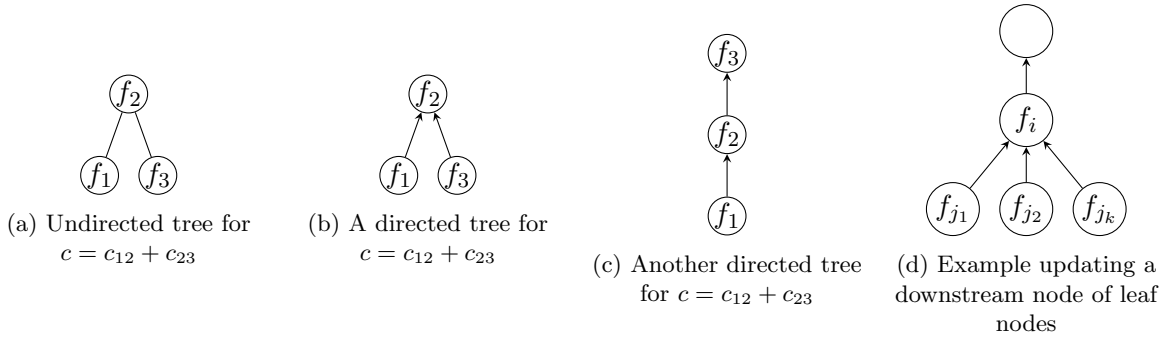


Figure 4: Following [subsection 4.1](#), directed trees play a key role in defining ascent directions and computing c -transforms. As shown by (b) and (c) however, there are multiple directed variants of any undirected tree.

4.2. Graphical Interpretation and General Dual Gradients. The undirected tree in [Figure 4a](#) represents the simple three-marginal problem considered above. Directed versions of this tree can be defined by choosing a single root node and ensuring that all edges in the tree point towards the root node. This is shown in [Figure 4b](#) for root node f_2 or in [Figure 4c](#) for root node f_3 . For either of these choices, the dual variable of the root node is given by the c -transform. In [subsection 4.1](#), readers may find the dual gradient [\(4.6b\)](#) is special, comparing with [\(4.4\)](#) and [\(4.6a\)](#), or even [\(2.6\)](#) in the two-marginal setting. In [\(4.6b\)](#) (see [Figure 4c](#)), the pushforward map S_f from marginal μ_2 to μ_3 is no longer induced by the c -transform of the dual variable f_2 . Instead, it is induced by $f'_2 = (f_2 - f_1^{c_{12}})^{c_{23}}$, which we refer to as a net potential. On one hand, for the optimal solution (f_1, f_2, f_3) , one may expect $\mu_2 = (S_{f_3})_{\#}\mu_3$, and by [\(4.5\)](#), we see how the net potential f'_2 is constructed. On the other hand, nodes with incoming edges will require using a net potential. Before applying c_{23} -transform, one need to obtain a new potential $f_2^{\text{new}} = f_2 - f_1^{c_{12}}$, which accounts for upstream information. [Lemma B.2](#) in the supplementary document provides a detailed discussion. Loosely speaking, unlike the two-marginal OT, the dual variables in the MMOT problem are no longer purely loading/unloading prices.

The gradients in [\(4.4\)](#) and [\(4.6\)](#) were obtained by comparing the MMOT dual problem to the sum of dual problems for independent two-marginal OT problems. This same process can also be employed for larger problems with an arbitrary number of marginal distributions so long as the MMOT cost a pairwise cost as in [\(A1\)](#).

Consider a directed tree with root node r and the functional [\(4.1\)](#) defines

$$I_r(f_1, \dots, f_{r-1}, f_{r+1}, \dots, f_m) \triangleq I(f_1, \dots, f_{r-1}, \left(\sum_{i \neq r} f_i\right)^c, f_{r+1}, \dots, f_m).$$

In this more general setting and $i \neq r$, the gradient of I_r with respect to f_i takes the form

$$(4.7) \quad \nabla_{\hat{H}^1} I_r(f_i) = (-\Delta)^{-1} \left(\mu_i - (S_{f'_i})_{\#} \mu_{N^+(i)} \right),$$

where the net potential f'_i at edge $(i, N^+(i))$ is (iteratively) defined by

$$(4.8) \quad f'_i = \left(f_i - \sum_{j \in N^-(i)} f'_j \right)^{c_{iN^+(i)}},$$

which is the difference between the dual variable at node i and the sum of upstream net potentials. [Figure 4d](#) illustrates the idea. If node i is a leaf node, the set of upstream nodes is empty $N^-(i) = \emptyset$ and the net potential is simply $f'_i = (f_i)^{c_{iN^+(i)}}$. Notice that this agrees with the gradients in [\(4.4\)](#) and [\(4.6\)](#) derived for the three marginal example in [subsection 4.1](#).

4.3. Gradient Ascent. The gradients defined by [\(4.7\)](#) provide a way to update each individual dual variable using gradient ascent while holding the other dual variables fixed, that is, a block coordinate ascent algorithm for the dual MMOT problem, except the root node. At iteration t of the gradient ascent algorithm, the dual variable at node i is updated using

$$f_i^{t+1} = f_i^t - \sigma \Delta^{-1} \left[\mu_i - (S_{f_i^t})_{\#} \mu_{N^+(i)} \right],$$

for a step size $\sigma \in \mathbb{R}$. As described in the previous section however, the dual variable at the root node is given by the c -transform $f_r = (\sum_{i \neq r} f_i)^c$. The following lemma provides a mechanism for efficiently computing this c -transform using the same net potentials used to define those gradients.

Lemma 4.1. *For a root node r and its upstream nodes $N^-(r)$, we have:*

$$(4.9) \quad f_r(x_r) = \sum_{i \in N^-(r)} f'_i(x_r).$$

Proof. When the rooted tree only consists of two layers, the root node and the leaf nodes. By $f_r = (\sum_{i \neq r} f_i)^c$ and the definition [\(4.8\)](#),

$$\begin{aligned} f_r(x_r) &= \inf_{\text{all } y_i} c(y_1, \dots, x_r, \dots, y_m) - \sum_{i \in N^-(r)} f_i(y_i) = \inf_{\text{all } y_i} \sum_{i \in N^-(r)} (c_{ir}(y_i, x_r) - f_i(y_i)) \\ &= \sum_{i \in N^-(r)} (\inf_{y_i} c_{ir}(y_i, x_r) - f_i(y_i)) = \sum_{i \in N^-(r)} f_i^{c_{ir}}(x_r) = \sum_{i \in N^-(r)} f'_i(x_r). \end{aligned}$$

When the rooted tree consists of more than two layers, we may first re-arrange

$$\begin{aligned} f_r(x_r) &= \inf_{\text{all } y_i} c(y_1, \dots, x_r, \dots, y_m) - \sum_{i \neq r} f_i(y_i) \\ &= \inf_{\text{all } y_i} \sum_{i \in N^-(r)} \left[c_{ir}(y_i, x_r) - f_i(y_i) - \sum_{\substack{j \in \text{Tree}(i) \\ j \neq i}} f_j(y_j) + \sum_{(j,k) \in \text{Tree}(i)} c_{jk}(y_j, y_k) \right] \end{aligned}$$

$$= \sum_{i \in N^-(r)} \left[\inf_{y_i} \left(c_{ir}(y_i, x_r) - f_i(y_i) + \inf_{\substack{\text{all } y_j \\ j \in \text{Tree}(i)}} \left(\sum_{(j,k) \in \text{Tree}(i)} c_{jk}(y_j, y_k) - \sum_{\substack{j \in \text{Tree}(i) \\ j \neq i}} f_j(y_j) \right) \right) \right]$$

where we denote a rooted tree with root node r by $\text{Tree}(r) = (V, E)$. For simplicity, we slightly abuse notations: $e \in \text{Tree}(r)$ ($v \in \text{Tree}(r)$) means that an edge (a vertex) belongs to the tree with root node r . We can continue this work by re-arranging the infimum by subtrees, to get a nested infimum.

From the inside to the outside of the nested infimum, by noting (4.8) and (iteratively) defining $f_i^{\text{new}} = f_i - \sum_{j \in N^-(i)} f'_j$ from the leaf nodes towards the root, we obtain (4.9). ■

Combine all necessary ingredients above, we have [Algorithm 1](#).

Algorithm 1: Gradient ascent step on a rooted tree.

```

1 Function AscentStep( $(V, E)$ ,  $\{f_1, \dots, f_m\}$ ,  $\{\mu_1, \dots, \mu_m\}$ ,  $r$ ,  $\sigma$ )
   Data: A tree  $(V, E)$  with  $m$  nodes; the index  $r$  of the root node, potentials
            $\{f_1, \dots, f_m\}$  and measures  $\{\mu_1, \dots, \mu_m\}$  at each node; and a stepsize  $\sigma$ .
   Result: Updated values of  $\{f_1, \dots, f_m\}$ .

   /* Use a breadth-first search to compute the layer  $L_i$  of node  $i$ . */
2  $L_1, \dots, L_m = \text{BFS}(V, E, r)$ ;

   /* Find a run order  $k_1, \dots, k_m$  such that  $L_{k_s} \geq L_{k_t}$  for  $s < t$ . */
3  $[k_1, \dots, k_m] \leftarrow \text{reverse}(\text{argsort}([L_1, \dots, L_m]))$ ;

   /* Loop over nodes in graph. */
4 for  $i \leftarrow 1$  to  $m - 1$  do
   |   /* Update net potential. */
   |    $f'_{k_i} \leftarrow \left( f_{k_i} - \sum_{j \in N^-(k_i)} f'_j \right)^c$ ;
   |   /* Take gradient step. */
   |    $f_{k_i} \leftarrow f_{k_i} - \sigma \Delta^{-1} \left[ \mu_{k_i} - \left( S_{f'_{k_i}} \right)_{\#} \mu_{N^+(k_i)} \right]$ ;
7 end

   /* Set root potential to ensure potentials are admissible */
8  $f_{k_m} \leftarrow \sum_{j \in N^-(k_m)} f'_j$ ;

10 return  $\{f_1, \dots, f_m\}$ ;

```

4.4. A study on Wasserstein barycenter. Agueh and Carlier [AC11] introduced the Wasserstein barycenter problem:

$$(4.10) \quad \inf_{\mu \in \mathbb{P}(X)} \sum_{i=1}^m \frac{\lambda_i}{2} W_2^2(\mu_i, \mu)$$

for a given sequence of probability measures $(\mu_i) \subseteq \mathbb{P}(X)$ and positive weights (λ_i) . The minimizer μ is called as the *Wasserstein barycenter*. Without loss of generality, let's assume $\sum_{i=1}^m \lambda_i = 1$. Agueh and Carlier showed (4.10) is equivalent to a MMOT of Gangbo-Święch type cost $c(x_1, \dots, x_m) = \sum_{1 \leq i < j \leq m} \frac{\lambda_i \lambda_j}{2} |x_i - x_j|^2$. We summarize their theorems as follows.

Theorem 4.2 ([AC11]). *For any m -tuple $(x_1, \dots, x_m) \in (\mathbb{R}^d)^m$ and $(\lambda_1, \dots, \lambda_m)$ such that $\sum_{i=1}^m \lambda_i = 1$, let us define the (Euclidean) barycenter map $T : (\mathbb{R}^d)^m \mapsto \mathbb{R}^d$:*

$$T(x_1, \dots, x_m) = \sum_{i=1}^m \lambda_i x_i.$$

The optimal solution P to the MMOT of Gangbo-Święch type cost

$$(4.11) \quad \inf_{P \in \Gamma(\mu_1, \dots, \mu_m)} \int_{(\mathbb{R}^d)^m} \left(\sum_{1 \leq i < j \leq m} \frac{\lambda_i \lambda_j}{2} |x_i - x_j|^2 \right) dP(x_1, \dots, x_m)$$

induces the barycenter μ to (4.10) by

$$(4.12a) \quad \begin{aligned} \mu &= (T)_{\#} P; \\ &= \left(\sum_{j=1}^m \lambda_j T_j^1 \right)_{\#} \mu_1; \end{aligned}$$

$$(4.12b) \quad = (\text{id} - \frac{1}{\lambda_i} \nabla f_i)_{\#} \mu_i.$$

where (f_i) are dual variables to (4.11), and for $x = (x_1, \dots, x_m)$ P -almost everywhere,

$$x_i = T_i^1(x_1) \triangleq \nabla \left(\frac{1}{2} |\cdot|^2 - \frac{f_i}{\lambda_i} \right)^* \circ \nabla \left(\frac{1}{2} |\cdot|^2 - \frac{f_1}{\lambda_1} \right) (x_1).$$

Proof. The proof is due to [GS98]. For completeness, please see the supplemental document. We follow the discussion in [AC11] but in terms of the dual variables (f_i) , rather than the variables $g_i(x_i) = \frac{\lambda_i(1-\lambda_i)}{2} |x_i|^2 - f_i(x_i)$ used in the convex analysis. ■

5. Numerical Results.

5.1. Comparison with the back-and-forth method. We first compare our method with the back-and-forth method on the cost function $c = \sum_{i=1}^{m-1} \frac{1}{2} |x_i - x_{i+1}|^2$ as a benchmark. Applying the gluing lemma, the optimal objective value is $\frac{1}{2} \sum_{i=1}^{m-1} W_2^2(\mu_i, \mu_{i+1})$.

	separate BFM	Our Method
storage	$2(m-1)$	m
Laplace	$2(m-1)$	$m-1$
c -transform	$4(m-1)$	$m-1$

Table 1: Computational complexity per iteration

5.2. Root Node Cycling. In theory, one can fix the root node and only update it by the c -transform of the sum of all other dual variables. In experiments shown in Figure 5, we observe that by picking different root nodes in a cycle, it accelerates the convergence dramatically. In some sense, cycling root nodes forces the solution to be c -conjugate tuples.

This natural variant of Algorithm 1 is shown in Algorithm 2.

We test with a simple example with marginals created by rigid translation, as shown in Figure 5a. The cost function is given by $c(x_0, x_1, x_2, x_3) = |x_0 - x_1|^2 + |x_1 - x_2|^2 + |x_2 - x_3|^2$. As shown in Figure 5b, cycling the root nodes in different iterations converges much faster than fixed root node algorithm.

Algorithm 2: Cyclic gradient ascent.

Data: A tree (V, E) with m nodes; measures $\{\mu_1, \dots, \mu_m\}$ at each node.

Result: Optimal values of dual potentials $\{f_1^*, \dots, f_m^*\}$.

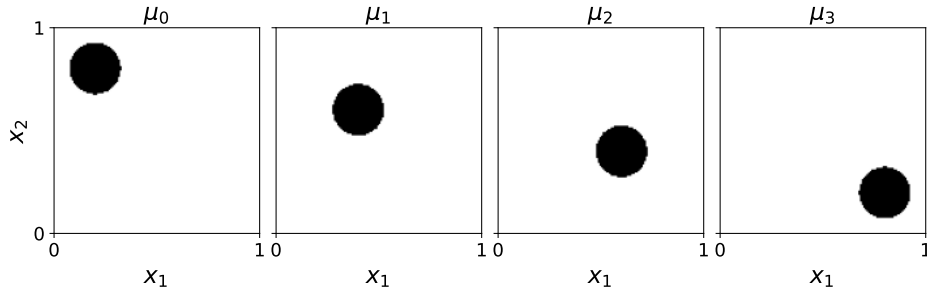
```

/* Initialize dual variables. */
1 for  $i \leftarrow 1$  to  $m$  do
2   |  $f_i \leftarrow 0$ ;
3 end

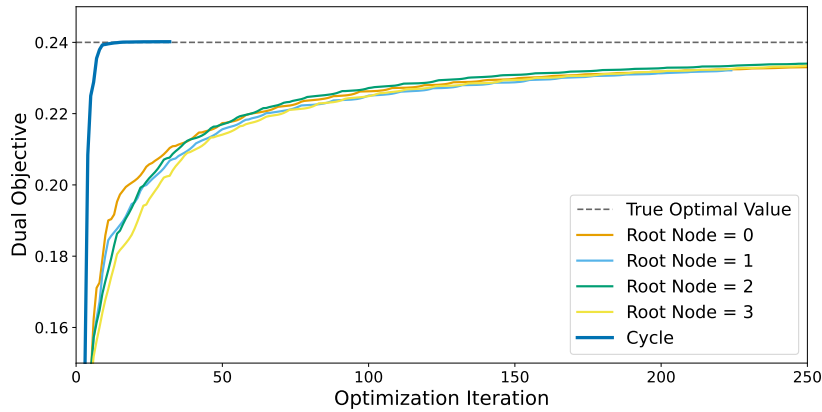
/* Initialize loop counter. */
4  $k \leftarrow 0$ ;
5 while not converged do
6   | /* Define root node. */
   |  $r \leftarrow (k \bmod m) + 1$ ;
   | /* Take gradient ascent step. */
   |  $\{f_1, \dots, f_m\} \leftarrow \text{AscentStep}((V, E), \{f_1, \dots, f_m\}, \{\mu_1, \dots, \mu_m\}, r, \sigma)$ ;
   | /* Increment loop index. */
   |  $k \leftarrow k + 1$ ;
7 end
10 return  $\{f_1, \dots, f_m\}$ ;

```

5.3. Wasserstein barycenter. Following our discussion in subsection 4.4, Figure 6 illustrates the pipeline of solving the Wasserstein barycenter problem via our algorithm. First, the Wasserstein barycenter problem corresponds to a complete undirected graph (see Figure 6a). Second, to solve (4.11) we first unroll this undirected graph with cycle by duplicating notes



(a) Marginal distributions used in root node cycling test.



(b) Optimization history for different values of the root node. Cycling through the root node results in dramatically faster convergence than setting root node to any single value.

Figure 5: The impact of cycling through the root node during the gradient steps. In this four-marginal example, the cost function is given by $c(x_0, x_1, x_2, x_3) = |x_0 - x_1|^2 + |x_1 - x_2|^2 + |x_2 - x_3|^2$, which can directly be mapped to a rooted tree without marginal duplication. The impact of using different directed trees during the gradient step is dramatic. With root node cycling, the algorithm converges in approximately 10 iterations, while the fixed-node gradient approach has not converged to the true value after 250 iterations.

(see Figure 6b). Last, after we pick a root node and add directionality (see Figure 6c), we may apply Algorithm 1 or Algorithm 2, to obtain the dual solutions $(\bar{f}_i)_{i=1}^{\frac{m(m-1)}{2}+1}$ to the new MMOT, and the optimal value to (4.11). To obtain the barycenter μ , we may use any dual variables f_i in (4.12b). However, except for the root node, the dual variables (f_i) to (4.11) are not necessary the same as the dual variables (\bar{f}_i) to the MMOT after we duplicate notes. It can be easier to use the dual variable at the root node in (4.12b).

In Figure 7, we use the same four marginals (a grid size of 412×412) “redcross”, “heart”, “tooth” and “duck” used in the POT (Python Optimal Transport) package [FCG⁺21], which are plotted at the four corners. All other plots are one of the Wasserstein barycenters, whose weights depend on their coordinates. After comparable computational times, our method pro-

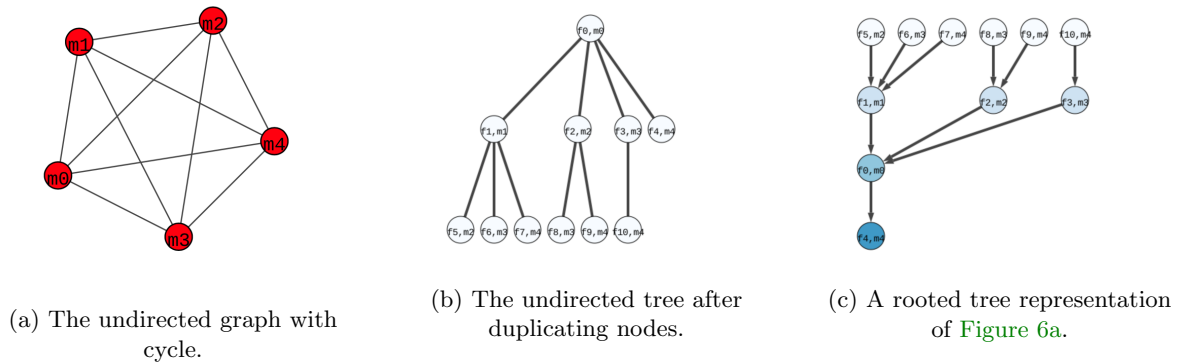


Figure 6: The pipeline to compute the Wasserstein barycenter via the MMOT approach. (a) is the corresponding undirected graph representation of the Gangbo-Świąch type cost. (b) is the undirected graph representation after “unrolling” (a) by duplicating the nodes. (c) is the rooted tree representation after picking a root node and is updated by [Algorithm 1](#).

vides much sharper interpolations (i.e., barycenters) than the regularization-based methods.

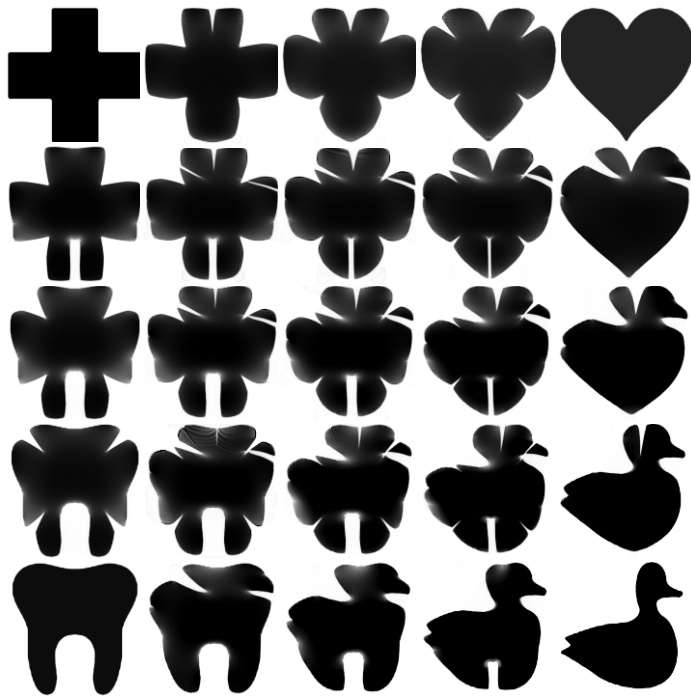


Figure 7: The Wasserstein barycenters of “readcross”, “heart”, “tooth” and “duck”. Any interpolated image (a weighted Wasserstein barycenter) is obtained by solving (4.10) and computing (4.12b). Those interpolated images show features from four marginals and have no diffusion effects.

6. Summary. We have presented a novel algorithm for the multimarginal optimal transport with pairwise cost functions. The exact (to within numerical tolerances) solutions can be used for applications which are sensitive to noises, and our results also provide a revisit and possible better understanding of previous results, including the regularized Wasserstein barycenter. The dual formulation on the graph may be scaled to complex marginals of fine details and large sizes of marginals. A python package, that works for arbitrary marginals and cost functions in a graph structure, with a quick guide, examples and API documents are provided and can be easily utilized for various purposes and researchers of diverse backgrounds.

As our method is inspired by the back-and-forth method, the gap between theoretical convergence analysis and numerical convergence observations inherits from BFM as well. It would be interesting to find a convergence result under mild assumptions. In the meanwhile, though our methods work for most cost functions in the literature of MMOT, it is natural to ask if our methods can be generalized to cost functions which are not the sum of pairwise functions, for example the determinant type of cost function [CN08]. Note that one of the motivation of such an assumption is due to the limitation of fast c -transforms. For pairwise cost function, the c -transform in high dimensions can be decomposed into nested 1D c -transforms, which can be obtained through fast algorithms of a divide-and-conquer type. As the c -transform is crucial to understand classical optimal transport theory, it maybe not be a coincidence that fast c -transforms are the key to numerical solutions.

Acknowledgments. To be added.

REFERENCES

- [ABS21] L. Ambrosio, E. Brué, and D. Semola. *Lectures on optimal transport*, volume 130 of *Unitext*. Springer, Cham, [2021] ©2021. La Matematica per il 3+2.
- [AC11] M. Agueh and G. Carlier. Barycenters in the Wasserstein space. *SIAM J. Math. Anal.*, 43(2):904–924, 2011.
- [ACB17] M. Arjovsky, S. Chintala, and L. Bottou. Wasserstein generative adversarial networks. In *International conference on machine learning*, pages 214–223. PMLR, 2017.
- [AG13] L. Ambrosio and N. Gigli. A user’s guide to optimal transport. In *Modelling and optimisation of flows on networks*, volume 2062 of *Lecture Notes in Math.*, pages 1–155. Springer, Heidelberg, 2013.
- [BB00] JD. Benamou and Y. Brenier. A computational fluid mechanics solution to the Monge-Kantorovich mass transfer problem. *Numer. Math.*, 84(3):375–393, 2000.
- [BCC⁺15] JD. Benamou, G. Carlier, Ma. Cuturi, L. Nenna, and G. Peyré. Iterative Bregman projections for regularized transportation problems. *SIAM J. Sci. Comput.*, 37(2):A1111–A1138, 2015.
- [BCM08] M. Bernot, V. Caselles, and J.-M. Morel. The structure of branched transportation networks. *Calc. Var. Partial Differential Equations*, 32(3):279–317, 2008.
- [BFO14] JD. Benamou, B. D. Froese, and A. M. Oberman. Numerical solution of the optimal transportation problem using the Monge-Ampère equation. *J. Comput. Phys.*, 260:107–126, 2014.
- [Bre89] Y. Brenier. The least action principle and the related concept of generalized flows for incompressible perfect fluids. *J. Amer. Math. Soc.*, 2(2):225–255, 1989.
- [Bre91] Y. Brenier. Polar factorization and monotone rearrangement of vector-valued functions. *Comm. Pure Appl. Math.*, 44(4):375–417, 1991.
- [Bre08] Y. Brenier. Generalized solutions and hydrostatic approximation of the Euler equations. *Physica D: Nonlinear Phenomena*, 237(14-17):1982–1988, 2008.
- [CFHR17] N. Courty, R. Flamary, A. Habrard, and A. Rakotomamonjy. Joint distribution optimal transportation for domain adaptation. In *Advances in Neural Information Processing Systems*,

- volume 30, 2017.
- [CMM⁺20] M. Caron, I. Misra, J. Mairal, P. Goyal, P. Bojanowski, and A. Joulin. Unsupervised learning of visual features by contrasting cluster assignments. In *Advances in Neural Information Processing Systems*, volume 33, pages 9912–9924, 2020.
- [CN08] G. Carlier and B. Nazaret. Optimal transportation for the determinant. *ESAIM Control Optim. Calc. Var.*, 14(4):678–698, 2008.
- [CP18] M. Cuturi and G. Peyré. Semidual regularized optimal transport. *SIAM Rev.*, 60(4):941–965, 2018. Revised reprint of “A smoothed dual approach for variational Wasserstein problems” [MR3466197].
- [Cut13] M. Cuturi. Sinkhorn distances: Lightspeed computation of optimal transport. In C.J. Burges, L. Bottou, M. Welling, Z. Ghahramani, and K.Q. Weinberger, editors, *Advances in Neural Information Processing Systems*, volume 26. Curran Associates, Inc., 2013.
- [dA82] A. de Acosta. Invariance principles in probability for triangular arrays of B -valued random vectors and some applications. *Ann. Probab.*, 10(2):346–373, 1982.
- [DBCC16] S. De, A. P. Bartók, G. Csányi, and M. Ceriotti. Comparing molecules and solids across structural and alchemical space. *Physical Chemistry Chemical Physics*, 18(20):13754–13769, 2016.
- [DMGN17] S. Di Marino, A. Gerolin, and L. Nenna. Optimal transportation theory with repulsive costs. In *Topological optimization and optimal transport*, volume 17 of *Radon Ser. Comput. Appl. Math.*, pages 204–256. De Gruyter, Berlin, 2017.
- [DPR18] A. Dessein, N. Papadakis, and J.-L. Rouas. Regularized optimal transport and the rot mover’s distance. *The Journal of Machine Learning Research*, 19(1):590–642, 2018.
- [Dud99] R. M. Dudley. *Uniform central limit theorems*, volume 63 of *Cambridge Studies in Advanced Mathematics*. Cambridge University Press, Cambridge, 1999.
- [EHJK20] F. Elvander, I. Haasler, A. Jakobsson, and J. Karlsson. Multi-marginal optimal transport using partial information with applications in robust localization and sensor fusion. *Signal Processing*, 171:107474, 2020.
- [FCG⁺21] R. Flamary, N. Courty, A. Gramfort, M. Z. Alaya, A. Boisbunon, S. Chambon, L. Chapel, A. Corenflos, K. Fatras, N. Fournier, L. Gautheron, N. Gayraud, H. Janati, A. Rakotomamonjy, I. Redko, A. Rolet, A. Schutz, V. Seguy, D. J. Sutherland, R. Tavenard, A. Tong, and T. Vayer. POT: Python Optimal Transport. *Journal of Machine Learning Research*, 22(78):1–8, 2021.
- [FHKC22] J. Fan, I. Haasler, J. Karlsson, and Y. Chen. On the complexity of the optimal transport problem with graph-structured cost. In Gustau Camps-Valls, Francisco J. R. Ruiz, and Isabel Valera, editors, *Proceedings of The 25th International Conference on Artificial Intelligence and Statistics*, volume 151 of *Proceedings of Machine Learning Research*, pages 9147–9165. PMLR, 28–30 Mar 2022.
- [FSV⁺19] J. Feydy, T. Séjourné, F.-X. Vialard, S. Amari, A. Trouvé, and G. Peyré. Interpolating between optimal transport and MMD using Sinkhorn divergences. In *The 22nd International Conference on Artificial Intelligence and Statistics*, pages 2681–2690. PMLR, 2019.
- [FZM⁺15] C. Frogner, C. Zhang, H. Mobahi, M. Araya, and T. A. Poggio. Learning with a Wasserstein loss. In *Advances in neural information processing systems*, volume 28, 2015.
- [Gan04] W. Gangbo. An introduction to the mass transportation theory and its applications. UCLA lecture notes, 2004.
- [GM96] W. Gangbo and R. J. McCann. The geometry of optimal transportation. *Acta Math.*, 177(2):113–161, 1996.
- [GPC18] A. Genevay, G. Peyré, and M. Cuturi. Learning generative models with Sinkhorn divergences. In *International Conference on Artificial Intelligence and Statistics*, pages 1608–1617. PMLR, 2018.
- [GS98] W. Gangbo and A. Świąch. Optimal maps for the multidimensional Monge-Kantorovich problem. *Comm. Pure Appl. Math.*, 51(1):23–45, 1998.
- [HRCK21] I. Haasler, A. Ringh, Y. Chen, and J. Karlsson. Multimarginal optimal transport with a tree-structured cost and the Schrödinger bridge problem. *SIAM J. Control Optim.*, 59(4):2428–2453, 2021.
- [HSZ⁺21] I. Haasler, R. Singh, Q. Zhang, J. Karlsson, and Y. Chen. Multi-marginal optimal transport

- and probabilistic graphical models. *IEEE Trans. Inform. Theory*, 67(7):4647–4668, 2021.
- [JL20] M. Jacobs and F. Léger. A fast approach to optimal transport: the back-and-forth method. *Numer. Math.*, 146(3):513–544, 2020.
- [Kel84] H. G. Kellerer. Duality theorems for marginal problems. *Z. Wahrsch. Verw. Gebiete*, 67(4):399–432, 1984.
- [KMT19] J. Kitagawa, Q. Mérigot, and B. Thibert. Convergence of a Newton algorithm for semi-discrete optimal transport. *J. Eur. Math. Soc. (JEMS)*, 21(9):2603–2651, 2019.
- [McC01] R. J. McCann. Polar factorization of maps on Riemannian manifolds. *Geom. Funct. Anal.*, 11(3):589–608, 2001.
- [MM16] Q. Mérigot and JM. Mirebeau. Minimal geodesics along volume-preserving maps, through semidiscrete optimal transport. *SIAM J. Numer. Anal.*, 54(6):3465–3492, 2016.
- [MSM03] F. Maddalena, S. Solimini, and J.-M. Morel. A variational model of irrigation patterns. *Interfaces Free Bound.*, 5(4):391–415, 2003.
- [NX22] A. Neufeld and Q. Xiang. Numerical method for feasible and approximately optimal solutions of multi-marginal optimal transport beyond discrete measures, 2022.
- [Pas11] B. Pass. Uniqueness and Monge solutions in the multimarginal optimal transportation problem. *SIAM J. Math. Anal.*, 43(6):2758–2775, 2011.
- [Pas15] B. Pass. Multi-marginal optimal transport: theory and applications. *ESAIM Math. Model. Numer. Anal.*, 49(6):1771–1790, 2015.
- [PR09] M. Peletier and M. Röger. Partial localization, lipid bilayers, and the elastica functional. *Arch. Ration. Mech. Anal.*, 193(3):475–537, 2009.
- [PVJ21] B. Pass and A. Vargas-Jiménez. Multi-marginal optimal transportation problem for cyclic costs. *SIAM J. Math. Anal.*, 53(4):4386–4400, 2021.
- [PWS⁺19] M. D. Parno, B. A. West, A. J. Song, T. S. Hodgdon, and D. T. O’Connor. Remote measurement of sea ice dynamics with regularized optimal transport. *Geophysical Research Letters*, 46(10):5341–5350, 2019.
- [Roc70] R. T. Rockafellar. *Convex analysis*. Princeton Mathematical Series, No. 28. Princeton University Press, Princeton, N.J., 1970.
- [San15] F. Santambrogio. *Optimal transport for applied mathematicians*, volume 87 of *Progress in Non-linear Differential Equations and their Applications*. Birkhäuser/Springer, Cham, 2015.
- [Sch19] B. Schmitzer. Stabilized sparse scaling algorithms for entropy regularized transport problems. *SIAM J. Sci. Comput.*, 41(3):A1443–A1481, 2019.
- [SDGP⁺15] J. Solomon, F. De Goes, G. Peyré, M. Cuturi, A. Butscher, A. Nguyen, T. Du, and L. Guibas. Convolutional Wasserstein distances: efficient optimal transportation on geometric domains. *ACM Transactions on Graphics (ToG)*, 34(4):1–11, 2015.
- [SK67] R. Sinkhorn and P. Knopp. Concerning nonnegative matrices and doubly stochastic matrices. *Pacific J. Math.*, 21:343–348, 1967.
- [SKA15] L. Saumier, B. Khouider, and M. Agueh. Optimal transport for particle image velocimetry: real data and postprocessing algorithms. *SIAM J. Appl. Math.*, 75(6):2495–2514, 2015.
- [TJK22] N. G. Trillos, M. Jacobs, and J. Kim. The multimarginal optimal transport formulation of adversarial multiclass classification, 2022.
- [Vil03] C. Villani. *Topics in optimal transportation*, volume 58 of *Graduate Studies in Mathematics*. American Mathematical Society, Providence, RI, 2003.
- [Xia03] Q. Xia. Optimal paths related to transport problems. *Commun. Contemp. Math.*, 5(2):251–279, 2003.
- [XZ21] Q. Xia and B. Zhou. The existence of minimizers for an isoperimetric problem with Wasserstein penalty term in unbounded domains. *Advances in Calculus of Variations*, 2021.
- [YESH18] Y. Yang, B. Engquist, J. Sun, and B. F. Hamfeldt. Application of optimal transport and the quadratic Wasserstein metric to full-waveform inversion. *Geophysics*, 83(1):R43–R62, 2018.

Appendix A. Supplementary contents to subsection 2.2.

Definition A.1 (Subdifferential). *The subdifferential $\partial\phi(x)$ is defined as:*

$$\partial\phi(x) \triangleq \{y \mid x' \cdot y - \phi(x') \text{ is maximal at } x' = x\}.$$

Definition A.2 (c -superdifferential). *The c -superdifferential is defined as:*

$$\partial^c f(x_1) \triangleq \{x_2 \mid c(x', x_2) - f(x') \text{ is minimal at } x' = x_1\}$$

Lemma A.3 and Theorem A.4 compare the Legendre transform with c -transform.

Lemma A.3 ([San15, ABS21]). *For $X_1 = X_2 = \mathbb{R}^d$,*

- (i) $\phi^{**} \leq \phi$, with equality if and only if ϕ is convex and lower semi-continuous;
- (ii) $f^{cc} \geq f$, with equality if and only if f is c -concave;
- (iii) For $c(x_1, x_2) = \frac{1}{2}|x_1 - x_2|^2$, $f(x_2)$ is c -concave if and only if $\phi(x_2) = \frac{1}{2}|x_2|^2 - f(x_2)$ is convex and lower semi-continuous. Moreover, $f^c(x_1) = \frac{1}{2}|x_1|^2 - \phi^*(x_1)$.
- (iv) For convex function ϕ and ϕ^* , we have

$$y \in \partial\phi(x) \iff \phi(x) + \phi^*(y) = x \cdot y \iff x \in \partial\phi^*(y).$$

- (v) $x_2 \in \partial^c f(x_1) \iff f(x_1) + f^c(x_2) = c(x_1, x_2) \iff x_1 \in \partial f^c(x_2)$.

Theorem A.4 ([Roc70, Gan04]).

- (i) *Given a strictly convex and lower semi-continuous function $\phi(x) : \mathbb{R}^d \mapsto \mathbb{R}$, then*

$$y = \nabla\phi^*(x)$$

is the unique maximizer to

$$\sup_y \langle x, y \rangle - \phi(y).$$

- (ii) *Given $c(x_1, x_2) = h(x_1 - x_2)$ for some strictly convex function h , assume $g(x_2)$ is a compactly supported continuous function, and $f(x_1) = g^c(x_1)$. If f is differentiable at x_1 , then*

$$x_2 \triangleq x_1 - (\nabla h)^{-1}(\nabla f(x_1)) = x_1 - \nabla h^*(\nabla f(x_1))$$

is the unique minimizer to

$$\inf_{x_2} c(x_1, x_2) - g(x_2).$$

That is, x_2 is the unique pre-image of x_1 under the mapping $\partial^c g$.

Appendix B. Supplementary Lemmas to subsection 4.1.

Lemma B.1. *Let $X_1, X_2, X_3 \subset \mathbb{R}^d$ be compact and convex domains and each measure $\mu_i \in \mathbb{P}(X_i)$ has a strictly positive density, and $c = c_{12} + c_{23}$ where $c_{12}(x_1, x_2) = h_1(x_1 -$*

$x_2), c_{23}(x_2, x_3) = h_2(x_2 - x_3)$ for some continuously differentiable and strictly convex functions h_1, h_2 . Define a functional

$$I((f_2 + f_3)^c, f_2, f_3) = \int_{X_1} (f_2 + f_3)^c(x_1) d\mu_1 + \int_{X_2} f_2(x_2) d\mu_2 + \int_{X_3} f_3(x_3) d\mu_3,$$

over the space of continuous function $f_2 : X_2 \mapsto \mathbb{R}, f_3 : X_3 \mapsto \mathbb{R}$. Then

$$\delta_{f_2} I(f_2; f_3) = \mu_2 - (S_{(f_2 - f_3^{c_{23}})^{c_{12}}}) \# \mu_1.$$

Proof. The proof follows the proof to lemma 3 in [JL20]. Please refer to Proposition 2.9 in [Gan04] for a detailed proof or refer to [GM96] for milder assumptions.

$$\begin{aligned} & \lim_{\varepsilon \rightarrow 0} \frac{I((f_2 + \varepsilon \xi + f_3)^c, f_2 + \varepsilon \xi, f_3) - I((f_2 + f_3)^c, f_2, f_3)}{\varepsilon} \\ &= \int_{X_1} \frac{(f_2(x_2) + \varepsilon \xi(x_2) + f_3(x_3))^c - (f_2(x_2) + f_3(x_3))^c}{\varepsilon} d\mu_1 + \int_{X_2} \xi(x_2) d\mu_2 \\ &= \int_{X_1} \frac{(f_2 - f_3^{c_{23}} + \varepsilon \xi)^{c_{12}} - (f_2 - f_3^{c_{23}})^{c_{12}}}{\varepsilon} d\mu_1 + \int_{X_2} \xi(x_2) d\mu_2 \\ &= - \int_{X_1} \xi(S_{(f_2 - f_3^{c_{23}})^{c_{12}}})(x_1) d\mu_1 + \int_{X_2} \xi(x_2) d\mu_2 \\ &= - \int \xi d[(S_{(f_2 - f_3^{c_{23}})^{c_{12}}}) \# \mu_1] + \int \xi d\mu_2. \quad \blacksquare \end{aligned}$$

Lemma B.2. Let $X_1, X_2, X_3 \subset \mathbb{R}^d$ be compact and convex domains, and each measure $\mu_i \in \mathbb{P}(X_i)$ is absolutely continuous with respect to the Lebesgue measure. For $c(x_1, x_2, x_3) = c_{12}(x_1, x_2) + c_{23}(x_2, x_3)$, we have:

- If $(u_1, v_1), (u_2, v_2)$ are optimal loading/unloading prices to the OT under cost c_{12}, c_{23} respectively, then $(f_1, f_2, f_3) = (u_1, v_1 + u_2, v_2)$ is the Kantorovich potential to the MMOT under the cost $c(x_1, x_2, x_3)$.
- If (f_1, f_2, f_3) is the Kantorovich potential to the MMOT under the cost $c(x_1, x_2, x_3)$, then $(u_1, v_1) = (f_1, f_1^{c_{12}}), (u_2, v_2) = (f_2 - f_1^{c_{12}}, f_3)$ are optimal loading/unloading prices to the OT under cost c_{12}, c_{23} respectively.

Proof. Given a probability measure $P \in \mathbb{P}(X_1, X_2, X_3)$, we define $P_1(A) = \int_{A \times X_2 \times X_3} dP$ and $P_{1,2}(A \times B) = \int_{A \times B \times X_3} dP$. On one hand

$$\begin{aligned} & \inf_{P \in \Gamma(\mu_1, \mu_2, \mu_3)} \int c_{12}(x_1, x_2) + c_{23}(x_2, x_3) dP \\ &= \inf_{P \in \Gamma(\mu_1, \mu_2, \mu_3)} \int c_{12}(x_1, x_2) dP_{1,2} + \int c_{23}(x_2, x_3) dP_{2,3} \\ &= \inf_{Q^1 \in \Gamma(\mu_1, \mu_2)} \int c_{12}(x_1, x_2) dQ^1 + \inf_{Q^2 \in \Gamma(\mu_2, \mu_3)} \int c_{23}(x_2, x_3) dQ^2 \\ \text{(B.1)} \quad &= \sup_{u_1 + v_1 \leq c_{12}} \int u_1 d\mu_1 + \int v_1 d\mu_2 + \sup_{u_2 + v_2 \leq c_{23}} \int u_2 d\mu_2 + \int v_2 d\mu_3; \end{aligned}$$

On the other hand,

$$(B.2) \quad \begin{aligned} & \inf_{P \in \Gamma(\mu_1, \mu_2, \mu_3)} \int c_{12}(x_1, x_2) + c_{23}(x_2, x_3) dP \\ &= \sup_{f_1 + f_2 + f_3 \leq c} \int f_1 d\mu_1 + \int f_2 d\mu_2 + \int f_3 d\mu_3. \end{aligned}$$

Given a tuple (u_1, v_1, u_2, v_2) that achieves the maximum in (B.1), we define $f_1 = u_1, f_2 = v_1 + u_2, f_3 = v_2$, then

$$f_1(x_1) + f_2(x_2) + f_3(x_3) = u_1(x_1) + v_1(x_2) + u_2(x_2) + v_2(x_3) \leq c_{12}(x_1, x_2) + c_{23}(x_2, x_3)$$

is an admissible solution to (B.2).

$$(B.1) = \int u_1 d\mu_1 + \int (v_1 + u_2) d\mu_2 + \int v_2 d\mu_3 = \int f_1 d\mu_1 + \int f_2 d\mu_2 + \int f_3 d\mu_3 \leq (B.2).$$

Since (B.1) = (B.2), the tuple (f_1, f_2, f_3) is a maximizer to (B.2).

Given a tuple (f_1, f_2, f_3) that achieves the maximum in (B.2), we define $u_1 = f_1, v_1 = f_1^{c_{12}}, u_2 = f_2 - f_1^{c_{12}}, v_2 = f_3$.

We first show that (u_1, v_1, v_2, u_3) is an admissible solution to (B.1). By definition, we just need to show that $u_2(x_2) + v_2(x_3) = f_2(x_2) - f_1^{c_{12}}(x_2) + f_3(x_3) \leq c_{23}(x_2, x_3)$. By the duality theory, $f_2(x_2) = (f_1 + f_3)^c = f_1^{c_{12}}(x_2) + f_3^{c_{23}}(x_2)$. Thus

$$\begin{aligned} f_1^{c_{12}}(x_2) + f_3^{c_{23}}(x_2) = f_2(x_2) = v_1(x_2) + u_2(x_2) &\implies u_2(x_2) = f_3^{c_{23}}(x_2) \\ &\implies u_2(x_2) = v_2^{c_{23}}(x_2), \end{aligned}$$

thus $u_2(x_2) + v_2(x_3) \leq c_{23}(x_2, x_3)$. As a result, (u_1, v_1, v_2, u_3) is an admissible solution to (B.1). Analogously the above, it is the maximizer to (B.1) as well. \blacksquare

Corollary B.3. *Given a sequence of Polish spaces with their probability measures $(X_i, \mu_i)_{i=1}^m$. For a fixed j , $(X_{m+1}, \mu_{m+1}) \triangleq (X_j, \mu_j)$. For any $i \neq j$, let $P^{(m)} \in \Gamma(\mu_1, \dots, \mu_m)$ and $P_{ij}^{(m)} \in \Gamma(\mu_i, \mu_{m+1})$. There exists a probability measure Q such that $Q \in \Gamma(\mu_1, \dots, \mu_{m+1})$.*

Proof. Let $S_1 = X_1 \times \dots \times X_m$ associated with a probability measure $P^{(m)}$. Let $S_2 = X_{m+1}$ associated with a probability measure μ_{m+1} . Let $T_1 = X_i, T_2 = X_j$ and $\lambda = P_{ij}^{(m)} \in \mathbb{P}(T)$. We define the projection map $\phi_1 : S_1 \mapsto T_1$ and the identity map $\phi_2 : S_2 \mapsto T_2$. Then

$$\begin{aligned} (\phi_1)_\# \nu_1 &= (\phi_1)_\# P^{(m)} = \mu_i = (\mathbf{Proj}_1)_\# P_{ij}^{(m)} = (\mathbf{Proj}_1)_\# \lambda, \\ (\phi_2)_\# \nu_2 &= (\phi_2)_\# \mu_{m+1} = \mu_j = (\mathbf{Proj}_2)_\# P_{ij}^{(m)} = (\mathbf{Proj}_2)_\# \lambda. \end{aligned}$$

By Lemma 3.2, there exists a $Q \in \mathbb{P}(S_1 \times S_2)$, such that:

$$\begin{aligned} (\mathbf{Proj}_1)_\# Q = \nu_1 = P^{(m)} &\implies (\pi_i)_\# Q = \mu_i \quad \text{for all } 1 \leq i \leq m, \\ ((\phi_1 \circ \mathbf{Proj}_1, \phi_2 \circ \mathbf{Proj}_2))_\# Q = \lambda = P_{ij}^{(m)} &\implies (\pi_{m+1})_\# Q = \mu_{m+1}. \end{aligned} \quad \blacksquare$$

Lemma B.4. *Given Polish spaces (X_i) , measures $\mu_i \in \mathbb{P}(X_i)$ and transport plans $P \in \Gamma(\mu_1, \mu_2)$ and $Q \in \Gamma(\mu_2, \mu_3)$, there exists a measure $\gamma \in \mathbb{P}(X_1 \times X_2 \times X_3)$ such that $\gamma_{1,2} = (\mathbf{Proj}_{1,2})\#\gamma = P$ and $\gamma_{2,3} = (\mathbf{Proj}_{2,3})\#\gamma = Q$.*

Proof. By the disintegration of measures we can write

$$\begin{aligned} P(A_1 \times A_2) &= \int_{A_2} P(A_1 | x_2) d\mu_2(x_2); \\ Q(A_2 \times A_3) &= \int_{A_2} Q(A_3 | x_2) d\mu_2(x_2), \end{aligned}$$

for some family of probability measures $P(\cdot | x_2) \in \mathbb{P}(X_1)$ and $Q(\cdot | x_2) \in \mathbb{P}(X_3)$.

Define $\gamma \in \mathcal{M}(X_1 \times X_2 \times X_3)$ by

$$\gamma(A_1 \times A_2 \times A_3) = \int_{A_2} P(A_1 | x_2) Q(A_3 | x_2) d\mu_2(x_2).$$

Then

$$\gamma(A_1 \times A_2 \times X_3) = \int_{A_2} P(A_1 | x_2) Q(X_3 | x_2) d\mu_2(x_2) = \int_{A_2} P(A_1 | y) d\mu_2(x_2) = P(A_1 \times A_2). \quad \blacksquare$$

Appendix C. Proof to subsection 4.4.

Proof to Theorem 4.2. [AC11] consider the equivalence between:

$$(C.1a) \quad \sup \int \left(\sum_{1 \leq i < j \leq m} \lambda_i \lambda_j x_i x_j \right) dP;$$

$$(C.1b) \quad \inf \sum_{i=1}^m \int g_i d\mu_i \quad \text{subject to} \quad \sum_{i=1}^m g_i \geq \sum_{1 \leq i < j \leq m} \lambda_i \lambda_j x_i x_j.$$

We considered

$$(C.2a) \quad \inf \int \sum_{1 \leq i < j \leq m} \frac{\lambda_i \lambda_j}{2} |x_i - x_j|^2 dP;$$

$$(C.2b) \quad \sup \sum_{i=1}^m \int f_i d\mu_i \quad \text{subject to} \quad \sum_{i=1}^m f_i \leq \sum_{1 \leq i < j \leq m} \frac{\lambda_i \lambda_j}{2} |x_i - x_j|^2.$$

These two sets of problems are equivalent under the change of variables:

$$g_i(x_i) = \frac{\lambda_i(1 - \lambda_i)}{2} |x_i|^2 - f_i(x_i).$$

The optimal condition to (C.1) is for P -a.e. $x = (x_1, \dots, x_m)$

$$\nabla g_i(x_i) = \lambda_i \sum_{j \neq i} \lambda_j x_j$$

$$\begin{aligned} \iff \nabla \left(\frac{\lambda_i}{2} |\cdot|^2 + \frac{g_i}{\lambda_i} \right) (x_i) &= \sum_{j=1}^m \lambda_j x_j = \nabla \left(\frac{\lambda_1}{2} |\cdot|^2 + \frac{g_1}{\lambda_1} \right) (x_1) \\ \iff x_i &= \nabla \left(\frac{\lambda_i}{2} |\cdot|^2 + \frac{g_i}{\lambda_i} \right)^* \circ \nabla \left(\frac{\lambda_1}{2} |\cdot|^2 + \frac{g_1}{\lambda_1} \right) (x_1) \triangleq T_i^1(x_1). \end{aligned}$$

By the change of variables, the optimal condition to (C.2) is for P -a.e. $x = (x_1, \dots, x_m)$

$$\begin{aligned} \nabla f_i(x_i) &= \lambda_i(1 - \lambda_i)x_i - \lambda_i \sum_{j \neq i} \lambda_j x_j = \lambda_i(x_i - \sum_j \lambda_j x_j) \\ \iff \nabla \left(\frac{1}{2} |\cdot|^2 - \frac{f_i}{\lambda_i} \right) (x_i) &= \sum_j \lambda_j x_j = \nabla \left(\frac{1}{2} |\cdot|^2 - \frac{f_1}{\lambda_1} \right) (x_1) \\ \iff x_i &= \nabla \left(\frac{1}{2} |\cdot|^2 - \frac{f_i}{\lambda_i} \right)^* \circ \nabla \left(\frac{1}{2} |\cdot|^2 - \frac{f_1}{\lambda_1} \right) (x_1) = T_i^1(x_1). \end{aligned} \quad \blacksquare$$